Journal of Marine Research, 72, 243–290, 2014

Simple models for the heat flux from the Atlantic meridional overturning cell to the atmosphere

by M. Behl[1,2,3], D. Nof[1,4], and S. Van Gorder[1]

ABSTRACT

It has been suggested that a slowdown of the Atlantic meridional overturning cell (AMOC) would cause the Northern Hemisphere to cool by a few degrees. We use a sequence of simple analytical models to show that due to the nonlinearity of the system, the simplified heat flux from the modeled AMOC to the atmosphere above is so robust that even changes of as much as 50% in the present AMOC transport are not enough to significantly change the temperature of the outgoing warmed atmosphere (i.e., the fraction of the atmosphere warmed by the AMOC). Our most realistic model (which is still a far cry from reality) involves a warm ocean losing heat to an otherwise motionless and colder atmosphere. As a result, the compressible atmosphere convects, and the generated airflow ultimately penetrates horizontally into the surrounding air. The behavior of the system is attributable to four key aspects of the underlying physical processes: (1) convective atmospheric transport increases by warming the atmosphere, (2) the ocean is warmer than the atmosphere, (3) the surface heat flux is usually proportional to the temperature difference between the ocean and the atmosphere, and (4) the specific heat capacity of water is much larger than that of the air. Taken together, these properties of the system lead to the existence of a dynamic "asymptotic" state, a modeled regime, in which even significant changes in the AMOC transport have almost no effect on the ocean-atmosphere heat flux and the resulting outgoing atmospheric temperature. In the hypothetical limit of an infinitely large specific heat capacity of water, C_{pw} there is no change in either the atmospheric transport or the temperatures of the ocean and the atmosphere, regardless of how large the reduction in the AMOC transport is. Although our models may be too simple to allow for a direct application to the ocean and atmosphere, they do shed light on the processes in question.

Keywords. convection, AMOC, heat flux, asymptotic state, transport, atmosphere, ocean, temperature, heat capacity, conceptual models

1. Introduction

Heinrich events suggest that the variability of the Atlantic meridional overturning cell (AMOC; Fig. 1) leads to very dramatic changes in the Northern Hemisphere climate.

1. Department of Earth, Ocean and Atmospheric Sciences, The Florida State University, Tallahassee, FL 32306.
2. The Georgia Sea Grant College Program, The University of Georgia, Athens, GA 30602.
3. Corresponding author ***e-mail: mbehl@uga.edu***
4. Geophysical Fluid Dynamics Institute, The Florida State University, Tallahassee, FL 32306.

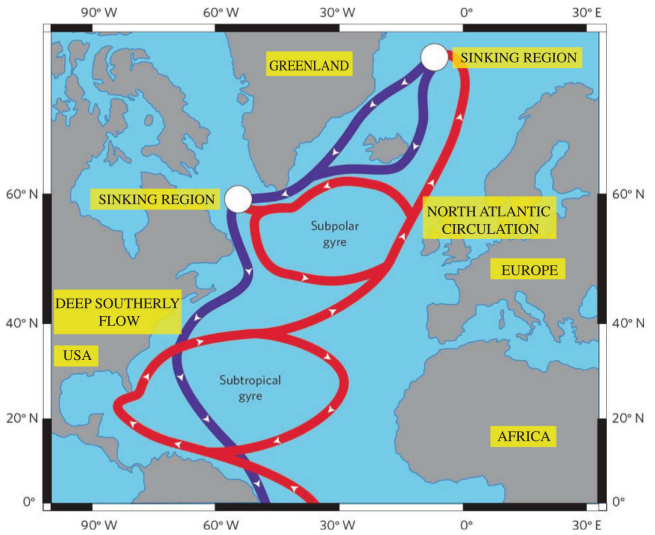

Figure 1. A schematic for the North Atlantic overturning circulation (adapted from De Boer, 2010). Warm surface water (red) flows northward and loses heat to the atmosphere before it sinks at the convection sites (white circles). Cold, dense water at the bottom (blue) generates a deep southerly flow.

The Intergovernmental Panel on Climate Change (IPCC) Fourth Assessment (2007) concluded that it is "very likely" (>90%) that there will be a slowdown of the AMOC during the 21st century. However, Zhang et al. (2011) argued against the IPCC projections, saying that even though the AMOC might have weakened from the 1960s to early 1970s, it has been strengthening from that time to the end of the last century. The 11 models used in the IPCC rely on reducing the AMOC transport using the familiar "hosing" procedure (i.e., adding freshwater to the surface of the North Atlantic, which reduces the salinity and, hence, the sinking rate).

Several attempts have been made to determine whether the AMOC transport has actually been reduced in the past 50 years. Bryden, Longworth, and Cunningham (2005) suggested—on the basis of five snapshot measurements made over five decades—that the AMOC had already slowed by 30% (>5–6 *Sv*, 1 $Sv = 10^6$ $m^3 s^{-1}$). Their interpretation of slowing was strongly disputed because of the unknown size and frequency spectrum of the AMOC variability. Cunningham et al. (2007) suggested that the aliasing of seasonal AMOC anomalies has accounted for a large part of the inferred slowdown. Similarly, using observations from the Meridional Overturning Variability Experiment (MOVE), Send, Lankhorst, and Kanzow (2011) reported that the AMOC has declined by 3 *Sv* over a 10-year period (January 2000 to January 2009). Further background on the AMOC can be found in the reviews of Lozier et al. (2008, 2010) and Lozier (2010, 2012).

Modeling studies by Schmittner, Latif, and Schneider (2005), IPCC (2007), and Hu et al. (2009) suggested a significant slowing down of the AMOC in response to increased greenhouse gas concentrations in the atmosphere. In addition, salinities in the North Atlantic ocean have decreased considerably since the mid-1960s (Curry and Mauritzen 2005). The northward flow of the AMOC provides approximately one-quarter of the global meridional heat transport (Kanzow et al. 2007). Srokosz et al. (2012) pointed out that 1 petawatt ($PW = 10^{15}$ W) of heat carried by the AMOC is released to the atmosphere between 26° N and 50° N, and has important implications on the climate of the North Atlantic region. Most global climate models predict that Europe should cool within this century as a response to an AMOC reduction. Such cooling has been attributed to a large decrease in the heat flux to the atmosphere.

Here, we use simple models to examine both the magnitude and direction of the atmospheric and oceanic temperature changes associated with a reduction of the AMOC. Although our models are simplified so that they cannot be directly applied to the ocean and atmosphere, we shall argue that for the modeled parameter range relevant to the Atlantic, there exists a dynamic "asymptotic state" within which even large reductions in the AMOC transport do not cause any significant change in the atmospheric transport, the outgoing atmospheric temperature, and the heat flux from the AMOC to the atmosphere. With a decrease in AMOC transport, the rate at which the modeled ocean cools is faster than the rate at which the modeled atmosphere warms.

a. Background

Several attempts have been made to assess the effect of the slowing down of the AMOC on the temperature of the Northern Hemisphere. Most of these attempts are based on high-resolution global and local numerical models. Because these numerical models include many more processes than simple analytical models, it is very difficult to understand them without first isolating at least some of the processes. Also, the global numerical models (e.g., the models used for the IPCC Fourth Assessment) have oceanic resolution on the order of 50–100 km in the horizontal, with 30–50 levels in the vertical, whereas, in reality, spatial scales of a few kilometers are important for processes such as atmospheric convection. As with all models, the results of the global numerical models need to be questioned primarily because of the lack of complete observational data for the AMOC.

Aside from the original classical box models with or without convection (e.g., Colin de Verdière 2007 and the references given therein), there are not many simple models describing the variability of the AMOC. Nof, Van Gorder, and Yu (2011) examined the atmospheric response to the potential slowing down of the AMOC using an analytical approach similar to that of Sandal and Nof (2008), but with the relaxation of a key "closure condition" of Sandal and Nof asserting the equality of the ocean and atmospheric mass transports. Without specifying any relationship between the two transports, Nof, Van Gorder, and Yu (2011) analyzed several scenarios for the response of the atmosphere to a slowdown of the AMOC

and concluded that if there is a significant reduction (say 50%) in the heat flux from the ocean to the atmosphere, then there will most likely (in their words, "under most circumstances that we can envision" [Nof, D., S. Van Gorder, and L. Yu. 2011; 13: Section 5.1]) be atmospheric warming in the immediate vicinity of the convection region. However, they also found, in the particular case in which the atmospheric transport is independent of the AMOC (a scenario that they considered to be exceptional and "probably irrelevant to nature" [Nof, D., S. Van Gorder, and L. Yu. 2011; 14: Section 5.2]), that both the atmosphere and ocean cool weakly, with only a minimal reduction in the heat flux from the ocean to the atmosphere. In contrast to Nof, Van Gorder, and Yu (2011), we shall argue here that what they considered to be an exception to the rule is actually typical of the response to changes in the AMOC when the system is in a regime that we call the "asymptotic state."

We present here a more complete and dynamically based investigation of the response of the atmosphere to changes in the AMOC than that done by either Sandal and Nof (2008) or Nof, Van Gorder, and Yu (2011). Using buoyancy-driven convection equations for the atmosphere (i.e., rather than the closure condition relating the ocean and atmospheric mass transports used in Sandal and Nof [2008]) and bulk formulas for the surface fluxes, we examine the atmospheric and oceanic temperature changes that result from a slowing down of an idealized AMOC. In order to focus on the atmospheric response to changes in the AMOC transport, we eliminate ocean convection and freshwater forcing processes and simply take the ocean transport to be our independent variable. As just mentioned, we find that there is a realistic regime, which we call the asymptotic state, in which no matter what reduction in transport the AMOC suffers, the changes in the atmosphere are minimal. Specifically, even for a significant (50%) reduction in the AMOC transport, there is a very small atmospheric and oceanic cooling, which is associated with both a small reduction in the atmospheric transport and the heat flux from the ocean to the atmosphere.

b. Present study

We propose here a series of four nonlinear analytical models (Fig. 2) as increasingly more realistic analogues for the atmospheric response to changes in the AMOC. Our series of models cover a wide range of scales and have very different physical configurations (from buildings enclosing pools of water to open "no-roof" atmosphere–ocean areas the size of the North Atlantic), but despite this we shall see that they all have a similar qualitative behavior. In particular, they all have a regime that we call the asymptotic state, suggesting that the asymptotic state concept is a robust feature of a wide range of air–sea interactions that are based on bulk formula surface exchange processes and buoyancy-driven atmospheric convection.

Our simplest conceptual "hot spring" model (Fig. 2, upper left panel; and Fig. 3) is similar to the "passive cooling" structures used in traditional ancient Persian (Fig. 4) and other (e.g., Roman) cultures. In ancient times, architects were obliged to rely on natural processes to render the inside condition of the buildings pleasant. Bahadori (1978) described the passive

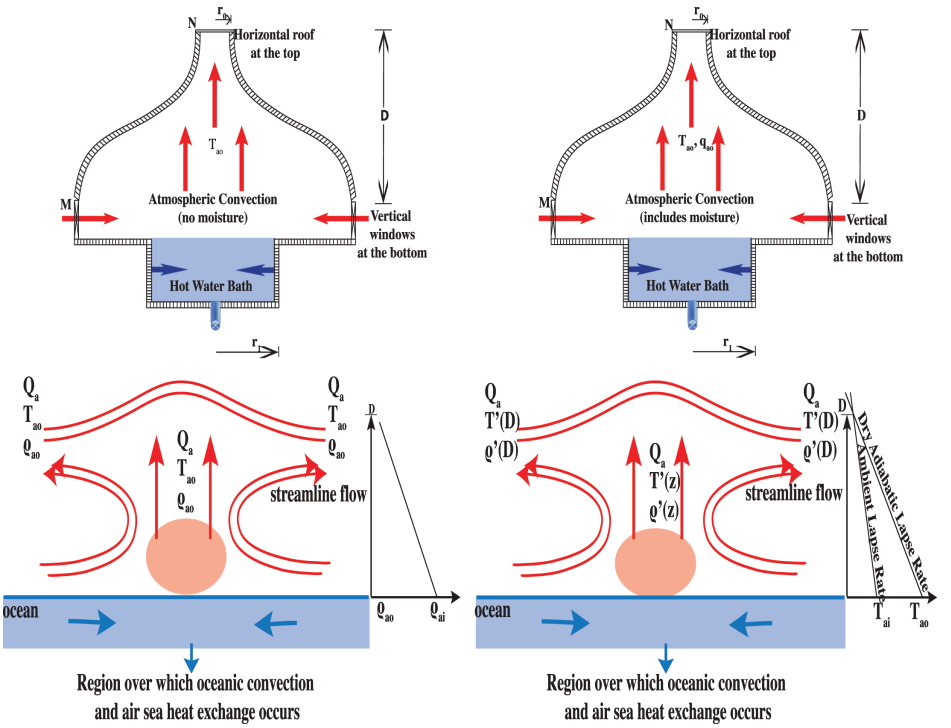

Figure 2. The four models with an increasing level of complexity. The simplest model (upper left) consists of a hot spring covered by a bell-shaped bathhouse with open windows (or vents) located at the peak of the roof and around the periphery of the building near the ground. The air is warmed by the hot water bath, rises, and escapes through the vent in the roof, drawing air in through the windows near the ground. At the next level of complexity, the air also absorbs moisture from the hot bath, which enhances the atmospheric convection (upper right). The next two levels involve expanding the scale and removing the roof, replacing it with an open stratified atmosphere (lower two panels). In the oceanic scale, incompressible atmosphere–ocean model (lower left), atmospheric convection occurs between warm ocean and cool atmosphere in the same way as the hot spring model without moisture. For simplicity, the atmosphere is assumed to be incompressible (i.e., the ambient density and temperature are linear functions of height). Within the convection region, the process is assumed to be adiabatic. In our last model, the compressible atmosphere ocean model (lower right), we improve the incompressible atmosphere ocean model by adding compressibility to the atmosphere. The ambient temperature is now a linear function of height, and again, within the convection region, the process is assumed to be adiabatic. The basic idea of the analogy between models represented in the upper and lower panels is that the flow within the hot bath, representing the Atlantic meridional overturning cell (AMOC), warms the air in the building (representing the atmosphere above the AMOC) causing it to convect. The plots on the right-hand side of the two lower panels show the atmospheric vertical density and temperature profiles in the environment (labeled ρ_{ai} and T_{ai} at the surface) and in the convection region (labeled ρ_{ao} and T_{ao} at the surface).

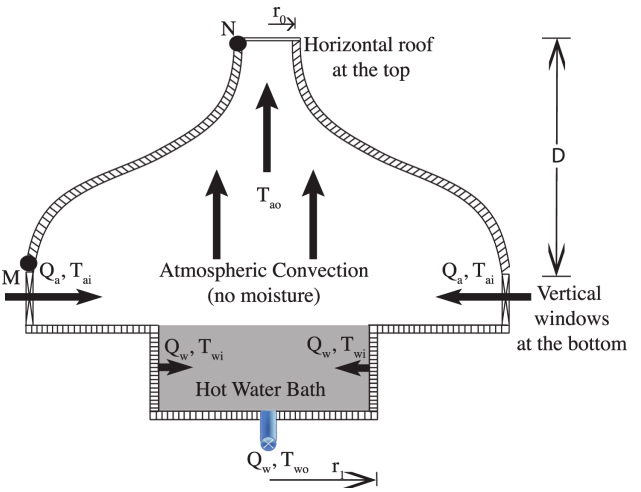

Figure 3. The hot spring model without moisture. A round hot bath is situated in a bell-shaped bathhouse with an opening or window at the peak of the roof and an assembly of vertical open windows located around the outer periphery near the ground. The round hot bath, into which water from a hot spring is diverted, has a flow from its periphery to a sink at its center. While flowing toward the sink, the hot water heats the air above it, which convects, draws air into the bathhouse through the vertical windows near the ground (M), and escapes the bathhouse through the round horizontal window in the roof (N). In this simple hot spring model, we do not account for any changes in the density of the air due to moisture. The volume flux of the air flowing through the bathhouse is Q_a, and that of the water flowing through the hot bath is Q_w. The height of the round window (with radius r_0) is D. The radius of the round hot bath is r_1. The temperatures of the incoming air and water are T_{ai} and T_{wi}. The temperature of the outgoing water is T_{wo}.T_{ao} is the nearly uniform temperature of the air inside the bathhouse away from the immediate vicinity of the hot bath where the heat exchange occurs.

cooling systems that the Persians used to ventilate their homes and keep them naturally cool in hot summer months (Fig. 4). These systems were constructed by opening vents in the roof of a building containing fountains or pools of water on the ground. Such an arrangement allows warm and moist air to rise and escape through the roof vents during the night when the outside air is cooler than the inside air. The rising warm and moist air reduces the pressure at the base of the building, drawing in cold air through vents located around the periphery of bottom of the building. More will be said about that shortly.

We develop our simplest conceptual hot spring model using principles similar to this passive cooling. However, in our analogy to the AMOC, we will shift the focus from the cooling provided by the drawing of nighttime air into the building to the heating of that air by the hot spring, which causes the convection driving the airflow through the building. At the other end of the spectrum, our most realistic (compressible) atmosphere–ocean convection model (Fig. 2, lower right panel) incorporates the familiar urban heat island (initially formulated by Lu et al. 1997, Parts I and II). A key feature, common to

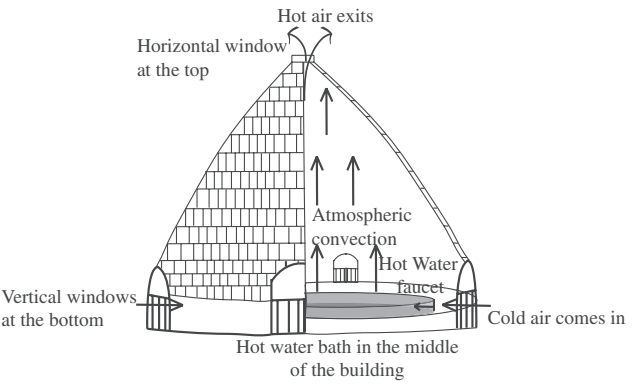

Figure 4. Schematic of a building with an ancient Persian "passive cooling" architecture. The dynamics of its heat exchange are analogous to our hot spring models shown in the upper panels of Figures 2 and 3. The cutaway reveals the hot water bath in the middle of the building and the vertical windows at the bottom through which the air is drawn into the building. There is a vent at the peak of the roof through which the air exits. In this passive cooling system, convection is due to both the heat and moisture exchange between the hot water and the cold air.

all our models is that both the atmospheric transport and air temperature decrease with a decrease in the heat flux to the atmosphere. The heat flux is proportional to the temperature difference between the ocean and the atmosphere; therefore, a reduction in the heat flux implies a reduction in both the temperature of the atmosphere and the temperature difference of the ocean and the atmosphere. Because the ocean is about 10°C–20°C warmer than the atmosphere, this can only be achieved when the rate at which the ocean cools is faster than the rate at which the atmosphere warms, resulting in a small reduction in the air–sea temperature difference. The heat capacity of water is four times that of air, so one might intuitively expect that this requirement would severely restrict the reduction in temperature of both the atmosphere and the ocean in response to a reduction in the AMOC that is also associated with a reduced ocean–atmosphere heat flux. In fact, as we shall see, for an infinitely large specific heat capacity of water, neither the atmosphere warms nor the ocean cools, no matter how large the reduction in our modeled AMOC.

Our four models are as follows: a building-size hot spring model without moisture; a hot spring model with moisture; an incompressible atmosphere–ocean convection model, set in the open ocean with no roof; and lastly, a compressible atmosphere–ocean convection model (Fig. 2). We discuss the detailed dynamics of each of these models in Section 2. The rest of this document is organized in three sections. We begin with a discussion of the most simple conceptual hot spring model without moisture (Fig. 2, upper left panel) in Section 2a. In this model, the surface saturation specific humidity q_s^* and the surface Bowen ratio Be (i.e., the ratio of sensible to latent heat flux) are taken to be constants. (Note that all the symbols and abbreviations are conventional and are defined in Appendix 2; some

Table 1. Comparison of the hot spring model with and without moisture (with roof).

	Hot spring model without moisture	Hot spring model with moisture
Saturation specific humidity	$q_s^* = q^*(T_w) = const$ $q^*(T_a) = q_s^* + [C_{pa}/L_e B_e](T_a - T_w)$ $B_e^{-1} = [(L_e/C_{pa})\partial q^*/\partial T]^{T=T_w} = const$	$q_s^* = q^*(T_w) = 1.61 \times 10^6 e^{-Le/R_v T_w}$ $q^*(T_a) = 1.61 \times 10^6 e^{-Le/R_v T_a}$
Unknown parameters	T_{wo}, T_{ao}, Q_a	$T_{wo}, T_{ao}, Q_a, q_{ao}, R_{Ho}$
Known parameters	T_{wi}, T_{ai}, Q_w, R_H	$T_{wi}, T_{ai}, Q_w, R_{Hi}$
Atmospheric convection equation	$Q_a = a[2gD\alpha(T_{ao} - T_{ai})]^{1/2}$	$Q_a = a[2gD\{\alpha(T_{ao} - T_{ai}) + \beta(q_{ao} - q_{ai})\}]^{1/2}$

are defined in the text as well.) The relative humidity R_H is also taken to be a constant. Next, we add moisture to the conceptual hot spring model (Fig. 2, upper right panel) and relax our simplifying constraints on q_s^*, Be, and R_H in order to assess the impact of those simplifications on the convective system (Section 2b). In this model, moisture is included in the equation of state, q_s^* is no longer constant but is a nonlinear function of temperature, the linearization of the atmospheric saturation specific humidity utilizing Be is eliminated, and the relative humidity is an unknown (see Table 1). Even though q_s^* is a variable, we find that there is no qualitative change in the behavior of the system. This is the justification for again making them constants in our last two "atmosphere–ocean" models. In Section 2c, we construct a more realistic atmosphere–ocean convection model. Rather than being set in a building with a roof, this ocean-scale incompressible model (Fig. 2, lower left panel) is open at the top. We do not consider the contribution of moisture to the equation of state and justify these simplifications based on the similarity of the hot spring models with and without moisture. The ambient density and temperature are linear functions of height, and within the convection region, the process is assumed to be adiabatic. Hence, temperature and density are conserved as parcels convect upward. Lastly, we improve this model by taking into account the compressibility of the atmosphere (Section 2d). In the compressible atmosphere–ocean convection model, the ambient temperature is a linear function of height, and again, within the convection region, the process is assumed to be adiabatic. Now the potential temperature of parcels is conserved as they convect upward. This compressible atmosphere–ocean model (Fig. 2, lower right panel) is our most realistic model of the air–sea interaction and atmospheric convection system.

The results for all our models are summarized in Section 3, which begins with the hot spring model without moisture (Sections 3a and 3b), the hot spring model with moisture (Section 3c), the incompressible atmosphere–ocean model (Section 3d), and lastly, the compressible atmosphere–ocean model (Section 3e). Note that, due to the nonlinearity of the system, it is very difficult to solve our model equations in a straightforward fashion

because, even though the equations are algebraic, they are quite complicated. In most cases, to make our mathematical calculations tractable, we take the atmospheric mass transport to be known and the water mass transport to be an unknown (the reverse of the point of view adopted in the physical model). For this reason, we present the mathematical details of all the solutions in Appendix 1 rather than the text. Within the text, the presentation follows our physical point of view in which the atmosphere responds to a reduction in the water mass flux (analogous to a reduction in the mass flux of the AMOC) rather than the other way around. This approach is taken merely for mathematical convenience. Note that we explain all our graphical results (Section 3) in the conventional left-to-right manner; that is, instead of explaining the system response to a decrease in AMOC reduction, we explain the system response to an increase in AMOC response. We conclude with a thorough discussion (Section 4) of the asymptotic state, factors affecting asymptotic state, and model weaknesses.

2. Dynamics of conceptual models

a. Hot spring model without moisture

Consider our most simple "hot spring model" (Fig. 3, Table 1), in which a round hot bath is situated inside a bell-shaped bathhouse with a round horizontal window in its roof and an assembly of vertical windows along the periphery near the ground. The round hot bath (into which water from a hot spring situated nearby is diverted) has a flow from its periphery to a sink in its center. This flow is artificially controlled. While flowing toward the center, the hot water releases heat to the air, which, as a result, convects, draws air into the bathhouse through the vertical windows near the ground, and escapes the bathhouse through the round window at the top. As the air flows from the bottom to the top of the bathhouse, its velocity increases and the pressure decreases. The heat loss from the hot water to the air is parameterized by the standard bulk formulas for sensible and latent heat fluxes.

This model is conceptually analogous to the AMOC with the water in the hot bath and the air in the bathhouse (respectively) playing the roles of the convecting ocean and atmosphere in the North Atlantic convection region. The question that we wish to address here is what happens when one reduces the flow of the hot water through the hot bath. Does that warm or cool the air inside the bathhouse and, if so, how much? This question is, in principle, analogous to the question, what is the atmospheric response to a reduction in the AMOC transport? We shall see that the answer is not at all simple.

i. Atmospheric convection. To determine whether the air inside the bathhouse (Fig. 3) cools or warms when the water flow is reduced, we examine the heat exchange that occurs between the hot water and the cool air inside the bathhouse. The volume flux of the air flowing through the bathhouse is Q_a, and that of the water flowing through the pool is Q_w. Let the height of the round window at the top, whose radius is r_0, be D, and the radius of the round hot bath

be r_1. (The area of the top window, πr_0^2, is denoted by a.) The velocity of the air at the top is W_D, the density of the air inside the bathhouse is ρ, and the constant density of the air outside (i.e., ambient density) is ρ_a. If $P_M$is the outside hydrostatic pressure at (the lower entrance of the bathhouse, Fig. 3), then the outside hydrostatic pressure at N (the upper exit) is

$$P_N = P_M - \rho_a g D. \tag{1}$$

It is next assumed that both the heat and moisture exchange occurs in the immediate vicinity of the pool at the bottom of the bathhouse so that the density ρ (and the temperature) inside the bathhouse is approximately constant. Away from the immediate vicinity of the bottom (where there is horizontal motion), and along a vertical line at the center of the bathhouse, the nonhydrostatic vertical equation of motion (in conventional notation) is

$$w\partial w/\partial z + g = \frac{-1}{\rho}\partial P/\partial z,$$

which can be integrated from the bottom to the top to give

$$W_D^2/2 + gD = \frac{-1}{\rho}(P_N - P_M).$$

Using (1) to express the pressure differences on the Right-Hand-Side (RHS), we immediately get

$$W_D = (2g'D)^{1/2}, \tag{2}$$

where $g' = g(\rho_a - \rho)/\rho_a$.

Note that $(\rho_a - \rho)/\rho$ was replaced with $(\rho_a - \rho)/\rho_a$ in the above expression, and that expressions identical or similar to (2) are often used in various engineering chimney calculations.

Next, let T_{ai} be the temperature of the incoming air (temperature at the surface) at M, and T_{ao} the temperature of the outgoing air (temperature at the top of the convecting region) at N. To be clear, we note that in line with our assumption above, T_{ao} is the temperature everywhere inside the bathhouse, except in the immediate vicinity of the pool at the bottom where the heat and moisture exchange occurs. The linearized equation of state (around T_{ai}) is

$$\rho = \rho_a \{1 - \alpha(T_{ao} - T_{ai})\}, \tag{3}$$

where $\alpha(\simeq 1/T_{ai})$ is the thermal expansion coefficient for air. For simplicity, we do not account for moisture in the equation of state. This will be taken into account in our next model (Section 2b). Combining (2) and (3) gives the air volume flux as

$$Q_a = a\{2gD\alpha(T_{ao} - T_{ai})\}^{1/2}. \tag{4}$$

Leaving this information aside for a moment, we now proceed with the general derivation and solution.

ii. Atmosphere–ocean heat exchange for the no-precipitation case ($\overline{P} = 0$). Assuming that there is sensible but no latent heating of the air (i.e., no precipitation within the bathhouse itself), the atmospheric heat gain equation and the hot bath heat loss equation are

$$\rho_a Q_a C_{pa}(T_{ao} - T_{ai}) = A\overline{F}_S = A\rho_a C_{pa} c_S U_{10}\,[\{(T_{wo} + T_{wi}) - (T_{ao} + T_{ai})/2\}], \quad (5)$$

$$\rho_w Q_w C_{pw}(T_{wi} - T_{wo}) = A(\overline{F_S + F_L}) = A\rho_a C_{pa} U_{10}(c_S + c_L R_H/Be)[\{(T_{wo} + T_{wi}) - (T_{ao} + T_{ai})/2\}] + A\rho_a c_L Le U_{10} q_S^*(1 - R_H), \quad (6)$$

where A is the area of the hot spring; ρ_w and ρ_a, the densities of water and air; C_{pa} and C_{pw}, the specific heat capacities of water and air; F_S and F_L, the sensible and latent heat fluxes; c_S and c_L, the fixed exchange coefficients; U_{10}, the fixed wind speed at 10 m above the surface; q_S^*, the fixed saturation specific humidity of the air at the surface of the water; Le, the latent heat of evaporation for water; R_H, the fixed relative humidity of the air; and Be, the fixed equilibrium Bowen ratio at the surface. The bars above the heat flux terms indicate that the variable in question is a mean quantity. The above heat flux parameterization follows the approach taken by Hartmann (1994) and Sandal and Nof (2008). Note that the atmospheric temperature at the surface is not fixed but changes from T_{ai} to T_{ao} as the cooler surface air flows over the warmer surface water. Only the incoming surface atmospheric temperature, T_{ai}, is held constant. T_{ao} is the outgoing surface temperature and is clearly indicated by the heat flux bulk formulas, which use $(T_{ai} + T_{ao})/2$ as the mean surface air temperature.

Relation (6) is the simplest bulk formula for the ocean heat loss. In reality, the latent heat flux is also sensitively dependent on the temperature (through the dependence of the saturation specific humidity on temperature). The quantities q_s^* and Be depend on the mean ocean temperature in a nonlinear, exponential fashion (Hartmann 1994). Specifically,

$$Be^{-1} \equiv (Le/C_{pa})(\partial q^*/\partial T), \quad (7)$$

where $(\partial q^*/\partial T) \approx q^*(T)\{Le/(R_v T^2)\}$, and R_v is the gas constant for water vapor,

$$q^*(T) \simeq 1.61 \times 10^6 e^{-Le/R_v T}. \quad (8)$$

In general, the Bowen ratio decreases exponentially with temperature because the exponential increase of saturation specific humidity on temperature far outweighs the inverse square of temperature. This nonlinear variation is included in our next model (Section 2b).

Because T_{wo} is unknown, we choose our fixed q_s^* and Be based on the incoming water temperature T_{wi}. Although qualitatively it makes no difference, this simplification does introduce some quantitative changes to the solution, as we shall see in our next model (Section 2c). Also, for simplicity, we assume that R_H and U_{10} are fixed, and the exchange coefficients, c_S and c_L, are independent of the surface temperature. Note that, given a fixed value of Q_w in the limit $U_{10} \to 0$, there is no convection, as should be the case.

The three unknowns Q_a, T_{ao}, and T_{wo} can be found using (4), (5), and (6). However, as mentioned in the Introduction, for mathematical simplicity, we reverse the problem by

taking Q_a as given and Q_w as an unknown. Obtaining the solution this way is much easier than the original problem, but the algebra is still quite complex. In order to simplify the presentation, we present only a rough outline here. The reader is referred to Appendix 1a (subsections i and ii) for the details of the solution and a full analysis of its implications.

We first rearrange (4) to obtain a solution for T_{ao} (equation [A1], Appendix 1a). Next, we substitute (A1) into (5) to obtain a solution for T_{wo} (A2). Lastly, we substitute (A1) and (A2) into (6) to solve for Q_w (A3). The results are presented in Section 3. Note that in this most simple conceptual hot spring model, there is no precipitation so that latent cooling of the hot bath means that the outgoing air is moister than the incoming air. We have neglected the effect of the additional moisture on the air density and the atmospheric convection in (3) and (4), but we will include it in our next model (Section 2b).

iii. The precipitation equals evaporation case ($\overline{P} = \overline{E}$). In the previous section, we considered the case in which the water loses both latent and sensible heat, but the air absorbs only the sensible heat. When the air absorbs both the sensible and the latent heat that is lost by the hot water (i.e., precipitation = evaporation), (5) becomes

$$\begin{aligned}\rho_a Q_a C_{pa}(T_{ao} - T_{ai}) &= A(\overline{F_S + F_L}) \\ &= A\rho_a C_{pa} U_{10}(c_S + c_L R_H/Be)[\{(T_{wo} + T_{wi}) - (T_{ao} + T_{ai})\}/2] \\ &\quad + A\rho_a c_L Le U_{10} q_s^*(1 - R_H). \end{aligned} \tag{9}$$

Because the right-hand sides of (6) and (9) are the same, we can write (as in Sandal and Nof 2008) the following equation that succinctly states that all the heat that is given up by the ocean is absorbed by the atmosphere:

$$\rho_w C_{pw} Q_w (T_{wi} - T_{wo}) = \rho_a C_{pa} Q_a (T_{ao} - T_{ai}). \tag{10}$$

Note that because the mean precipitation is equal to the evaporation, the moisture of the air is unchanged as it passes through the bathhouse. Therefore, in this case, the neglect of the effect of moisture on air density and atmospheric convection in (3) and (4) is justified.

However, because $T_{ao} > T_{ai}$, the relative humidity of the outgoing air must be lower than that of the incoming air, calling into question our assumption of constant R_H. If q_a is the specific humidity of the air at temperature T_a, then $q_a = q^*(T_a)R_H$, and because $q^*(T_a)$ is an increasing function, R_H must decrease to keep q_a unchanged when the air is heated. We verified our assumption that the decrease in R_H is small by setting $q_a = q^*(T_{ao})R_{Ho} = q^*(T_{ai})R_H$ and verifying that $(R_H - R_{Ho})/R_H = [1 - q^*(T_{ai})/q^*(T_{ao})]$ is small.

Using (4), (9), and (10), we wish to solve for Q_a, T_{ao}, and T_{wo} in terms of Q_w. The details are given in Appendix 1a (subsection iii), and the relevant results are presented in Section 3.

iv. Mass transport ratio ($\overline{P} = \overline{E}$ case). Using (10), the water and air temperature changes in response to a reduction in the water transport can be expressed in terms of the ocean/atmosphere mass transport ratio. To do so, we rewrite the water–air heat exchange equation (10),

$$\lambda\, C_{pw}(T_{wi} - T_{wo}) = C_{pa}(T_{ao} - T_{ai}), \tag{11}$$

where λ measures the (unknown) ratio of the water mass transport to that of the air,

$$\lambda = (\rho_w Q_w / \rho_a Q_a) > 0.$$

For any fixed λ, (11) immediately implies that when the ocean is cooled, the atmosphere warms. In Sandal and Nof (2008), the chosen closure condition was $\lambda = 1$, whereas in our hot spring model, λ is an unknown. (Note that λ is indicated by γ in Sandal and Nof [2008].)

b. Hot spring model with moisture

We now incorporate moisture into the most simple hot spring model (Fig. 2, upper right panel; and Table 1) by taking into account the nonlinear variation of q_s^* and *Be* ([7] and [8]). We will also allow the relative humidity of the air flowing over the hot bath to be altered by the air–water interaction, by specifying the incoming relative humidity R_{Hi} and taking the relative humidity of the outgoing air R_{Ho} to be an unknown.

i. Model derivation. When there is no precipitation, the latent cooling of the ocean reduces the density of the atmosphere by making it moister. We account for this by adding a moisture term to the equation of state. Let q_{ai} be the specific humidity of the air coming into the bathhouse, and q_{ao} the specific humidity of the air inside the bathhouse. The equation of state can be written as

$$\rho = \rho_a[1 - \alpha(T_{ao} - T_{ai}) - \beta(q_{ao} - q_{ai})], \tag{12}$$

where $\beta = [-(1/\rho)\partial\rho/\partial\rho]_{\rho=\rho_{ai}}$ is the "moisture expansion coefficient." For air, $\beta \simeq [(1 - \varepsilon)/\{q_{ai}(1 - \varepsilon) + \varepsilon\}] \approx (1 - \varepsilon)/\varepsilon = 0.608$, where $\varepsilon = 0.622$; is the ratio of the molecular weight of water vapor to that of the dry air. Combining (2) and (12) gives the atmospheric convection equation,

$$Q_a = a[2gD\{\alpha(T_{ao} - T_{ai}) + \beta(q_{ao} - q_{ai})\}]^{1/2}. \tag{13}$$

The net rate at which moisture is gained by the atmosphere is

$$\rho_a Q_a(q_{ao} - q_{ai}) = Q(\overline{E} - \overline{P}) = A\{(\overline{F}_L/Le) - \overline{P}\}.$$

Taking $\overline{P} = 0$, we write the conservation of moisture as

$$\rho_a Q_a(q_{ao} - q_{ai}) = A(\overline{F}_L/Le) = [A\rho_a c_L U_{10}/2][\{q^*(T_{wi}) - q_{ai}\} + \{q^*(T_{wo}) - q_{ao}\}]. \tag{14}$$

For ($\overline{P} = \overline{E}$), this equation reduces to $q_{ao} = q_{ai}$. In what follows, we keep the specific humidity q_a as a dependent variable and allow q^* to vary (nonlinearly) with temperature (according to [8]). The relative humidity of the outgoing air R_{Ho}, in terms of saturation specific humidity q^* and the specific humidity q_{ao} at that level, is

$$R_{Ho} = \{q_{ao}/q^*(T_{ao})\}. \tag{15}$$

There is both sensible and evaporative cooling of the ocean, so the ocean heat loss equation is

$$\begin{aligned}\rho_w C_{pw} Q_w (T_{wi} - T_{wo}) &= A(\overline{F_S + F_L}) \\ &= A\rho_a C_{pa} c_S U_{10}[\{(T_{wi} + T_{wo}) - (T_{ai} + T_{ao})\}/2] \\ &\quad + A\rho_a c_L Le U_{10}[\{(q^*(T_{wi}) + q^*(T_{wo})) - (q_{ai} + q_{ao})\}/2].\end{aligned} \tag{16}$$

The atmospheric heat gain equation is (5) for $\overline{P} = 0$ and (10) for $\overline{P} = \overline{E}$.

The results for the hot spring model with moisture are summarized in Section 3. It is on the basis of this strong similarity in the behavior of the hot spring models with and without moisture that we justify returning to the simplifications of the hot spring model without moisture for our more realistic atmosphere–ocean models in Sections 2c and 2d. Specifically, for both our incompressible and compressible atmosphere–ocean models, there will be no moisture considerations in either the equation of state or the atmospheric convection equation, and the latent heat fluxes will be parameterized in the same manner as (9), with constant q_s^*, Be, and R_H. With these simplifications, the mathematics in those models becomes tractable.

c. Incompressible atmosphere–ocean model

In our incompressible atmosphere–ocean convection model (Fig. 2, lower left panel; Table 2), we parameterize the air–sea interaction between the warm ocean and cool atmosphere in the same way as the hot spring model without moisture. As in both hot spring models, U_{10} is fixed, and the exchange coefficients c_S and c_L are assumed to be independent of the surface temperature. Unlike our small-scale conceptual hot spring models, however, there is now no roof separating the convecting air from the ambient atmosphere. This introduces an additional unknown, the height to which the convecting air rises before spreading horizontally into the ambient air, into the model (Fig. 2, lower left panel; Table 2).

In this model, the atmospheric convection is conceptually separated into two distinct phases. In the first phase, there is an exchange of heat between the ocean and the atmosphere as cool air flows horizontally over warm water toward the convection region. Initially, the (incoming) temperature T_{ai} and density ρ_{ai} of a surface air parcel match the surrounding environmental conditions at the surface. As the parcel moves across the warm ocean, it is heated to an outgoing temperature T_{ao}, and its density is reduced to ρ_{ao}. In the second phase, the heated and buoyant air rises adiabatically to a height where its density matches the density

Table 2. Comparison of incompressible and compressible atmosphere–ocean convection models (no roof).

	Incompressible atmosphere–ocean model		Compressible atmosphere–ocean model	
Saturation specific humidity	$q_s^* = q^*(T_w) = const$ $q^*(T_a) = q^*(T_w)$ $+ (C_{pa} L_e / B_e(T_w))(T_a - T_w)$ $B_e(T_w) = const$		$q_s^* = q^*(T_w) = const$ $q^*(T_a) = q^*(T_w)$ $+ (C_{pa} L_e / B_e(T_w))(T_a - T_w)$ $B_e(T_w) = const$	
Density variation	Environment $\rho(z) = \rho_{ai}(1 - \varphi z)$ Decreases with height	Convection region $\rho(z) = \rho_{ao}$ Constant with height	Environment $\rho(z)$ Decreases with height	Convection region $\rho(z)$ Decreases with height at a lower rate than the environment
Parameters	Unknown T_{wo}, T_{ao}, Q_a, D	Known $T_{wi}, T_{ai}, Q_w, \varphi$	Unknown T_{wo}, T_{ao}, Q_a, D	Known $T_{wi}, T_{ai}, Q_w, \gamma_D, \gamma$
Vertical velocity	$W_D = [gD\alpha(T_{ao} - T_{ai})]^{1/2}$		$W_D = [2gD\alpha(T_{ao} - T_{ai})]^{1/2}$	
Height to which the parcel rises	$D = (T_{ao} - T_{ai})/(\varphi/\alpha)$		$D = (T_{ao} - T_{ai})/(\gamma_D - \gamma)$	
Atmospheric convection	$Q_a = a\alpha(T_{ao} - T_{ai})(g/\varphi)^{1/2}$		$Q_a = a\alpha(T_{ao} - T_{ai})$ $\times [2g/\alpha(\gamma_D - \gamma)]^{1/2}$	

of the surrounding environment, at which point it spreads horizontally into the ambient air. The density and temperature vary linearly with height in the ambient atmosphere, but because we consider the process to be adiabatic in the convection region, the temperature and density are conserved as parcels convect upward. In order to simplify the convection model, we assume that, although the warm water (ocean) loses both the sensible and latent heat, the atmosphere is warmed only by sensible heat; that is, we consider only the case of no local precipitation ($\overline{P} = 0$).

i. Buoyancy forces on the rising parcel. Consider a linearly stratified static incompressible atmosphere whose representative ambient density is $\hat{\rho}_a$. The (positive and constant) vertical density gradient φ is

$$\varphi = -[1/\hat{\rho}_a][\partial \rho_a / \partial Z]. \tag{17}$$

A parcel of air is adiabatically displaced upward just like a solid "buoyant" ball, which oscillates about its equilibrium position. The characteristic frequency can be derived by considering the motion of this parcel, displaced vertically a small distance Δh from its

equilibrium height D without disturbing its environment. We equate the vertical acceleration of the parcel to the buoyancy, which is proportional to the vertical displacement of the parcel from its equilibrium height, and use (17) to get

$$d^2h/dt^2 = g\varphi(D - h), \tag{18}$$

where h is the height of the parcel above the ground.

ii. Vertical speed of the rising parcel. By definition, the speed of the buoyant parcel is $W \equiv dh/dt$, and therefore,

$$dW/dt = d^2h/dt^2 = g\varphi(D - h). \tag{19}$$

Applying the boundary conditions $W = 0, h = 0$ at $t = 0$ and $W = W_D, h = D$ at $t = T$ (the time it takes the parcel to rise from the ground to $h = D$), to (19) gives

$$W_D = D(g\varphi)^{1/2}, \tag{20}$$

for the speed of the parcel at $h = D$. In this solution, the displacement of the parcel from D is not small. The parcel oscillates from $h = 0$ to $h = 2D$ with period $\{2\pi/(g\varphi)^{1/2}\}$ and has maximum speed W_D at $h = D$. Nevertheless, we take W_D to be a representative speed for the parcel as it rises from the ground to $h = D$.

iii. Maximum height to which the parcel rises. The linearized equation of state is

$$\rho = \rho_{ai}[1 - \alpha(T - T_{ai})], \tag{21}$$

where T_{ai} and ρ_{ai} are the incoming ambient temperature and density of the air at the surface, and is the thermal expansion coefficient, $\alpha = [-(1/\rho)\partial\rho/\partial T]_{\rho=\rho_{ai}}$, which for air (neglecting compressibility) is given by $\alpha \simeq 1/T_{ai}$. Taking $\hat{\rho}_a$ in (17) to be the ambient density at the ground ρ_{ai} gives the ambient density profile

$$\rho_a(z) = \rho_{ai}(1 - \varphi z),$$

and substituting this into (17) gives the ambient temperature profile,

$$T_a(z) = T_{ai} + (\varphi/\alpha)z. \tag{22}$$

After the air is heated from its ambient temperature T_{ai} to T_{ao} by the warm water, it rises to a height where its temperature and density match the ambient temperature and density. Equating $T_a(z = D)$ to T_{ao} in (22) gives

$$\varphi = \alpha(T_{ao} - T_{ai})/D. \tag{23}$$

With Q_a, the atmosphere's volume flux, and a, the area of the convection region, we find from (23) that

$$D = (Q_a/a)/(g\varphi)^{1/2}. \tag{24}$$

iv. Atmospheric convection. Substituting (23) into (20) gives

$$W_D = \{Dga(T_{ao} - T_{ai})\}^{1/2}, \tag{25}$$

and finally, substituting $W_D = (Q_a/a)$ and then (24) into (25) gives the convection equation for an incompressible atmosphere,

$$Q_a = a\{Dg\alpha(T_{ao} - T_{ai})\}^{1/2} = a\alpha(g/\varphi)^{1/2}(T_{ao} - T_{ai}). \tag{26}$$

Note that although (26) differs formally from the atmospheric convection equation for the hot spring model without moisture (4) only by a factor of $\sqrt{2}$, D is now a part of the solution rather than a specified constant. Note that from (24) D increases with the strength of the atmospheric convection.

Using (5), (6), (24), and (26), one wishes to find the solutions for T_{ao}, T_{wo}, D, and Q_a for given Q_w. Again, for mathematical simplicity, we take Q_a to be given and solve for Q_w (see Appendix 1c). Rearranging (26) gives an expression for T_{ao} (A31). Next, we substitute (A31) into (5) to find T_{wo} (A32), and finally, we substitute (A31) and (A32) into (6) to obtain an expression for Q_w (A33). The details of these solutions and a discussion of the results are given in Appendix 1c (subsections i and ii). The relevant results in terms of our original problem (Q_w given, Q_a unknown) are in Section 3.

d. Compressible atmosphere–ocean model

The compressible atmosphere–ocean convection model (Fig. 2, lower right panel; Table 2) is our most realistic atmosphere–ocean convection model. It is similar to the incompressible atmosphere–ocean model; however, because of the compressibility of the atmosphere, the density and the temperature of the atmosphere now vary with height in both the ambient environment and in the convection region. Once again, q_s^*, Be, R_H, U_{10}, c_S, and c_L are constants, moisture is neglected in the equation of state, and there is no latent heating of the atmosphere ($\overline{P} = 0$). Following Hartmann (1994), we assume that the atmosphere obeys the ideal gas law and that air parcels in the convecting region rise adiabatically and adjust immediately to the surrounding hydrostatic pressure.

As in the incompressible atmosphere–ocean model (Section 2c), atmospheric convection is separated into two steps. First, a surface parcel of cool air, initially with the same thermodynamic state as the surrounding fluid at the surface, flows horizontally toward the convection region over the warm ocean. Its incoming temperature is T_{ai}, and as it moves

across the warm ocean, it is heated to an outgoing temperature T_{ao}, and its density is reduced. The warmed and buoyant parcel then rises to a height where its density matches the density of the surrounding environment.

i. Buoyancy of the rising parcel. The temperature of the environment surrounding the convection region is assumed to decrease linearly with height,

$$T(a) = T_{ai} - \gamma z, \tag{27}$$

where T_{ai} is the incoming (environmental) temperature at the surface, and γ the environmental lapse rate (ELR).

Because convecting parcels rise adiabatically in our model, the temperature in the convection region $T'(z)$ decreases at the dry adiabatic lapse rate, $\gamma_D = g/C_{pa}$. Thus, we have,

$$T'(z) = T_{ao} - \gamma_D z, \tag{28}$$

where T_{ao} is the temperature of the outgoing air as it leaves the surface. Neglecting horizontal motions away from (above) the surface, the vertical acceleration of the rising parcel is $\frac{dw}{dt} = w\frac{\partial w}{\partial z}$. Equating the buoyancy force per unit mass to the vertical acceleration of a rising parcel gives an equation for w, the vertical speed of the parcels,

$$dw/dt = w\partial w/\partial z = g(\rho - \rho')/\rho' = g\{T'(z) - T(z)\}/T(z). \tag{29}$$

where ρ' is density of a rising parcel, and ρ the density of its environment.

ii. Particle vertical velocity. Substituting (27) and (28) into (29) and integrating from zero to D gives an expression for W_D, the vertical velocity of a parcel at height D,

$$(W_D)^2/2 = g\int_0^D (T_{ao} - \gamma_D z)/(T_{ai} - \gamma z)dz - gD.$$

Evaluating the integral on the RHS and expanding the result for $\gamma D/T_{ai} = 1$ gives the simplified expression

$$W_D = \{2gD(T_{ao}/T_{ai} - 1)\}^{1/2} = \{2gD\alpha(T_{ao} - T_{ai})\}^{1/2}. \tag{30}$$

From (30), we see that the vertical velocity is a function of the air temperature gain and the height to which the parcel rises. Interestingly, this expression is identical to W_D for the hot spring model without moisture, except that, of course, D is now an unknown that, as we shall see next, is also determined by the air temperature gain.

iii. Maximum height to which the parcel rises. The parcel of air reaches its maximum speed when the buoyancy force becomes zero (i.e., when the density of the parcel becomes equal to the density of the ambient air). The plume ultimately (i.e., after overshooting) spreads horizontally at the same height. Because the ambient and convective pressures are equal, the temperature of the parcel must also match the temperature of the ambient air. The maximum height to which the parcel rises, D, is derived by equating the temperature of the rising parcel to the environmental temperature at $z = D$. Using (27), (28) gives $T_{ai} - \gamma D = T_{ao} - \gamma_D D$, and solving for D gives

$$D = (T_{ao} - T_{ai})/(\gamma_D - \gamma). \tag{31}$$

The constant γ_D is 9.8 K km^{-1}, and the average ELR defined by the International Civil Aviation Organization from sea level to 11 km is 6.49 K km^{-1}. Note that because $T_{ao} > T_{ai}$ and $\gamma_D > \gamma$, D is positive in (31), and W_D is real in (30).

iv. Atmospheric convection in the compressible atmosphere. Using (30) and (31), one obtains the following atmospheric convection equation for a compressible atmosphere:

$$Q_a = a(T_{ao} - T_{ai})[\{2g/T_{ai}\}\{1/(\gamma_D - \gamma)\}]^{1/2} = a\alpha(T_{ao} - T_{ai})[2g/\{\alpha(\gamma_D - \gamma)\}]^{1/2}. \tag{32}$$

Using the same approach that we employed earlier, (5), (6), (31), and (32) give solutions for T_{ao}, T_{wo}, D, and Q_w in terms of Q_a. Rearranging (32) gives an expression for T_{ao} (A36). Next, we substitute (A36) into (5) to obtain a solution for T_{wo} (A37). Lastly, substituting (A36) and (A37) into (6) gives us an expression for Q_w (A38). The details and discussion of this solution are presented in Appendix 1d (subsections i and ii). The relevant results for the original problem (i.e., known Q_w, unknown Q_a) are given in Section 3.

v. Size of the convection region. It is important to realize that in both the incompressible and the compressible ocean–atmosphere convection models, the area over which the convection takes place, a, is *smaller* than the area of the air–sea interaction region A. Employing the results of lab experiments on the so-called "heat-island problem," Lu et al. (1997) estimated the relation between the width of the plume $l_{\min}$ and the width of the heat island d to be given by

$$l_{\min} \geq 1.11(W_D/Nd)^{1/2}d, \tag{33}$$

where W_D is the vertical velocity in the plume and N is the stratification [$N = (g\alpha\gamma_D)^{1/2}$]. We used (33) to determine the "convection area" for both the incompressible and the compressible atmospheres by associating $l_{\min}$ with the diameter of the convection region $2r_0$, and d with the diameter of the air–sea interaction region $2r_1$. Typical values of vertical

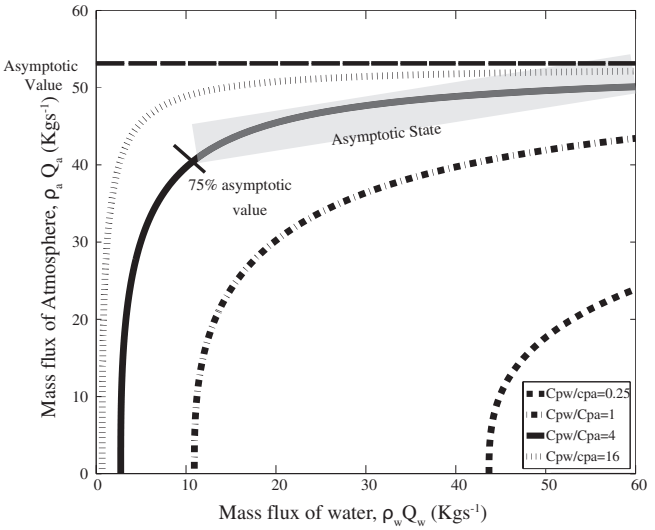

Figure 5. The atmospheric mass flux, $\rho_a Q_a$, as a function of the water mass flux, $\rho_w Q_w$, for hypothetical values of C_{pw}/C_{pa} in the hot spring model without moisture (with C_{pa} fixed and $\overline{P} = 0$). The asymptotic value of the mass flux $\rho_a \hat{Q}_a$ is approximately independent of C_{pa} and C_{pw}, which only control the onset of the asymptotic state $\rho_w \hat{Q}_w$. The onset of the asymptotic state (shaded regions) occurs earlier for high values of C_{pw}/C_{pa} than it does for low values. The parameters are $r_0 = 2.5\,m, r_1 = 50\,m, d = 13\,m, c_S = 0.0009, c_L = 0.00135, \rho_a = 1.5\,kgm^{-3}, \rho_w = 1,000\,kgm^{-3}, Le = 2.5 \times 10^6 Jkg^{-1}, g = 9.8\,ms^{-2}, T_{ai} = 10°C, T_{wi} = 25°C, U_{10} = 1.35\,ms^{-1}, q_s^* = 0.020, Be = 0.324$, and $R_H = 0.7$. For the $C_{pw}/C_{pa} = 4$ curve, $C_{pw} = 4,000\,Jkg^{-1}K^{-1}$, and $C_{pa} = 1004\,Jkg^{-1}K^{-1}$.

velocity W_D over the North Atlantic range between 8 and 15 m s^{-1}. For the North Atlantic, we found that $l_{\min} \geq 34$ km, $r_0 \geq 17$ km for $d = 2r_1 = 1{,}000$ km.

3. Results

a. Hot spring model without moisture ($\overline{P} = 0$)

As shown in Figure 5 and Appendix 1a (subsection ii), the mass flux of the air $\rho_a Q_a$ increases nonlinearly with an increase in the mass flux of the water $\rho_w Q_w$. For large $\rho_w Q_w$, $\rho_a Q_a$ approaches the asymptotic value $\rho_a \hat{Q}_a$ given approximately by (A11). In other words, for large enough $\rho_w Q_w$, $\rho_a Q_a$ and the other two unknowns T_{ao} and T_{wo} [expressed in terms of Q_a by (A1) and (A2)] change only weakly. Within this regime, even a large increase in $\rho_w Q_w$ does not cause the mass flux of the air $\rho_a Q_a$ to increase by a significant amount. We call this regime the "asymptotic state" (or "asymptotic regime") and define its lower limit or onset value $\rho_w \hat{Q}_w$ [given approximately by (A13)] as the value of $\rho_w Q_w$ where the mass flux of the air reaches 75% of its "asymptotic value" $\rho_a \hat{Q}_a$. For $(C_{pw}/C_{pa}) = 4$, this roughly corresponds to the point where the slope $(\rho_a/\rho_w)(\partial Q_a/\partial Q_w) = 1$. For our chosen hot spring parameters (caption of Fig. 5), $\rho_a \hat{Q}_a = 52.8\,kgs^{-1}$ and $\rho_w \hat{Q}_w = 9.9\,kgs^{-1}$. As

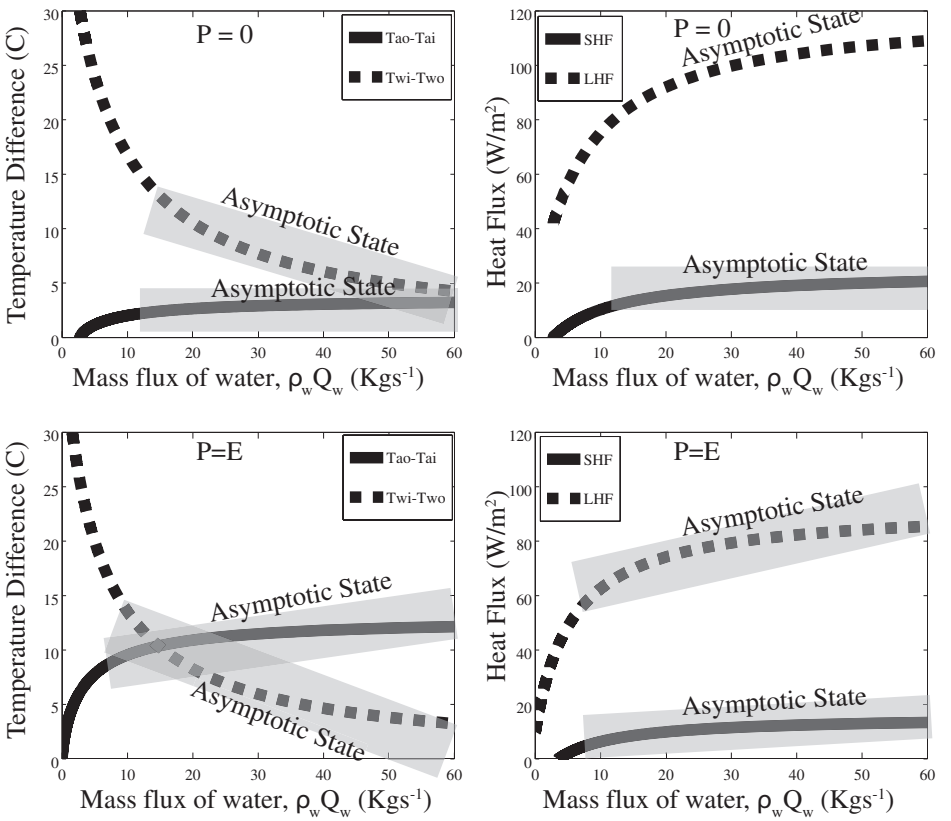

Figure 6. The water temperature loss and the air temperature gain as a function of the water mass flux, $\rho_w Q_w$ (left two panels), the mean sensible and latent heat fluxes as a function of the water mass flux (right two panels). All are shown for $C_{pw}/C_{pa} = 4$, $\overline{P} = 0$ (top two panels) and $\overline{P} = \overline{E}$ (bottom two panels) in the hot spring model without moisture. Shading indicates the asymptotic state. LHF and SHF refer to the latent heat flux and sensible heat flux, respectively.

shown in of Appendix 1a (subsection ii), and in the upper left panel of Figure 6, the air temperature gain ($T_{ao} - T_{ai}$) increases and the water temperature loss ($T_{wi} - T_{wo}$) decreases with an increase in the water mass flux ($\rho_w Q_w$). With an increase in ocean transport, the rate at which water cools is less than the rate at which the atmosphere warms ([A9] and Fig. 7). This results in an increase in water–air temperature difference. Because both the sensible and latent heat fluxes $\overline{F_S}$ and $\overline{F_L}$ are linear functions of the mean temperature difference between the ocean and the atmosphere (5), they both increase (Fig. 6, upper right panel; and Fig. 7). Within the asymptotic state, even an increase as large as 50% in $\rho_w Q_w$ does not cause T_{ao}, T_{wo}, $\overline{F}_S$, or $\overline{F}_L$ to increase by any significant amount. Although the asymptotic value itself, $\rho_a \hat{Q}_a$, does not depend on either C_{pa} or C_{pw} (see [A11]), the asymptotic onset value $\rho_w \hat{Q}_w$ depends on both the ratio C_{pa}/C_{pw} and C_{pw} (see [A13]). As

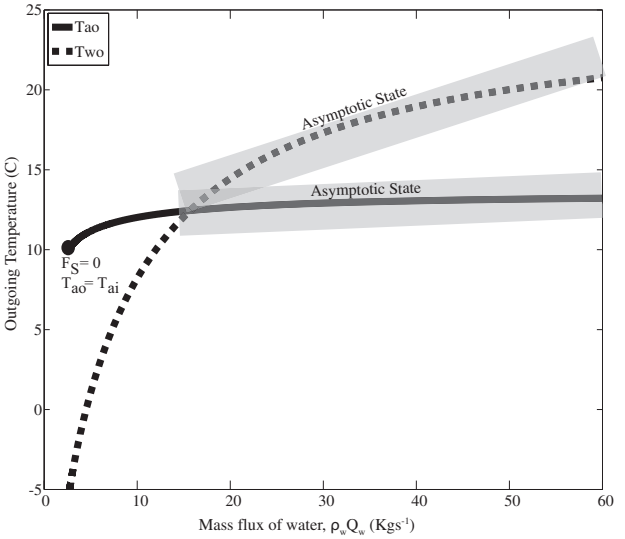

Figure 7. The outgoing air and water temperatures as a function of the water mass flux, $\rho_w Q_w$, for $C_{pw}/C_{pa} = 4$ in the conceptual hot spring model without moisture ($\overline{P} = 0$ case). Within the asymptotic state, changes in the outgoing water temperature are larger than changes in the outgoing air temperature. In response to a reduction of the mass flux of the water, the water in the hot bath cools more than the air above it. The solid dot is the cutoff point below which there are no (steady) solutions. At that point, sensible heat flux is zero and the air is no longer being cooled ($T_{ao} = T_{ai}$). As before, the shading indicates the asymptotic state.

illustrated in Figure 5, larger values of C_{pw} are associated with lower values of $\rho_w \hat{Q}_w$. In the hypothetical limit, $C_{pw} \to \infty$, the asymptotic onset value (marking the lower boundary of the asymptotic state) decreases to zero, and there is no change in any of the variables regardless of the change in Q_w (i.e., the system "completely asymptotes").

Atmospheric convection stops ($Q_a = 0$) at $Q_w = \{\rho_a c_L l e A U_{10} q_s^* (1 - R_H)\}/\{2\rho_w C_{pw}(T_{wi} - T_{ai})\}$. At this point, $(T_{ao} - T_{ai}) = 0$ and the mean sensible heat flux to the air is zero, but water is still being cooled by the latent heat flux (Fig. 5; Fig. 6, upper right panel; and Fig. 7). For smaller values of Q_w, there are no steady physical solutions.

b. Hot spring model without moisture ($\overline{P} = \overline{E}$)

The detailed solution is given in of Appendix 1a (subsection iii). Qualitatively, the results of the $\overline{P} = \overline{E}$ case are similar to the $\overline{P} = 0$ case, but the details are different. The asymptotic onset value $\rho_w \hat{Q}_w$ (given approximately by [A22], with $\delta = .75$) marks the beginning of asymptotic state and is lower than the $\overline{P} = 0$ case (A11). Put more simply, precipitation expands the "domain" of the asymptotic state. The asymptotic value $\rho_a \hat{Q}_a$, given approximately by (A19), is larger than the $\overline{P} = 0$ case (A11) due to the latent heating of the air caused by precipitation.

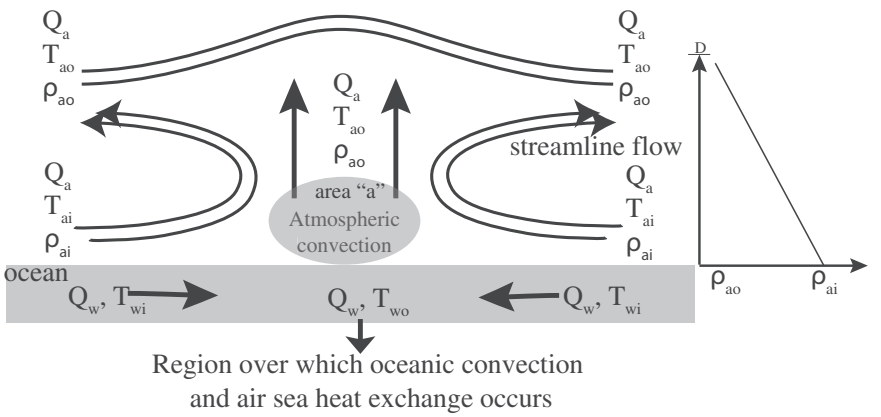

Figure 8. The incompressible atmosphere–ocean model. The heated air in the convection region rises adiabatically (conserving both its temperature and density) to a maximum height D, where its density matches that of the ambient air. The area (A) of the air–sea heat exchange region (with radius r_1) is much larger than convective area a (with radius r_0). The density, temperature of a cold parcel of incoming air is ρ_{ai}, T_{ai}, and ρ_{ao}, T_{ao}, is the density, temperature of a heated parcel of rising air. The plot on the right-hand side of the figure shows the atmospheric vertical density profile in the environment (labeled ρ_{ai} at the surface) and in the convection region (labeled ρ_{ao} at the surface).

Note that for $\overline{P} = \overline{E}$, the asymptotic value $\rho_a \hat{Q}_a$ is not independent of the specific heat capacities as it is in the $\overline{P} = 0$ case but depends on C_{pa}. Also note that to the order of the approximations in (A22), the asymptotic onset value $\rho_w \hat{Q}_w$ depends only on the ratio C_{pa}/C_{pw} and has no separate term dependent on C_{pw}. Again, higher values of C_{pw} are associated with lower asymptotic onset values, and in the hypothetical limit $C_{pw} \to \infty$, the system "completely asymptotes." For our chosen hot spring parameters (see caption of Fig. 5), $\rho_a \hat{Q}_a = 89.7\ kgs^{-1}$ and $\rho_w \hat{Q}_w = 4.4\ kgs^{-1}$.

As in the $\overline{P} = 0$ case, the air temperature gain ($T_{ao} - T_{ai}$) increases, and water temperature loss ($T_{wi} - T_{wo}$) decreases nonlinearly with an increase in $\rho_w Q_w$ (lower left panel of Fig. 6). Again, the warmer water is being cooled less than the cool air above it, resulting in an increase in the temperature difference between water and air, and hence an increase in both the sensible and latent heat fluxes (lower right panel of Fig. 6). However, within the asymptotic state, all these changes are insignificant. In contrast to the $\overline{P} = 0$ case, $Q_a = 0$ at $Q_w = 0$, and there are physical solutions for all $Q_w > 0$.

c. *Hot spring model with moisture*

Despite the mathematical complexity of the solution, the qualitative behavior of the solution is very similar to that of the hot spring model without moisture (there are only minor quantitative differences). For this reason, the solution itself will not be presented here, and the behavior of the model will only be summarized briefly. The details of the

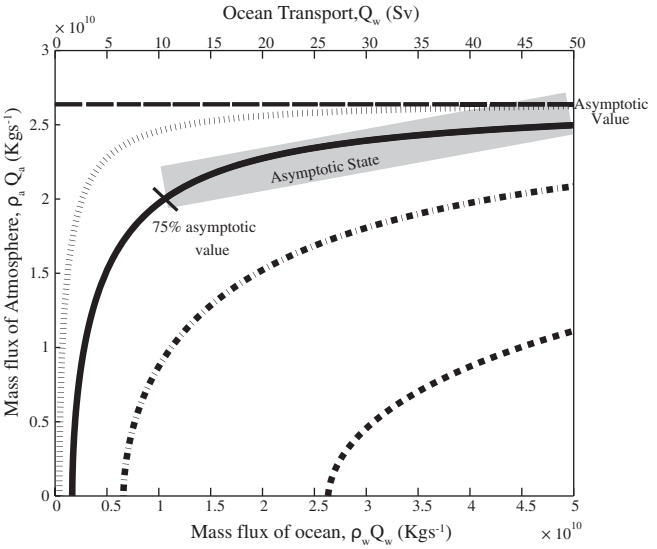

Figure 9. The atmospheric mass flux, $\rho_a Q_a$, as a function of the oceanic mass flux, $\rho_w Q_w$, for hypothetical values of C_{pw}/C_{pa} (with C_{pa} fixed) in the incompressible atmosphere–ocean model. The asymptotic value of the mass flux $\rho_a \hat{Q}_a$ is independent of C_{pa} and C_{pw}, which only control the onset of the asymptotic state $\rho_w \hat{Q}_w$. The onset of the asymptotic state (shaded regions) occurs earlier for high values of C_{pw}/C_{pa} than it does for low values. The parameters are $r_0 = 17.2\,km, r_1 = 500\,km, c_S = 0.0009, c_L = 0.00135, \rho_a = 1.5\,kgm^{-3}, \rho_w = 1,000\,kgm^{-3}, Le = 2.5 \times 10^6 Jkg^{-1}, g = 9.8\,ms^{-2}, T_{ai} = 10°C, T_{wi} = 30°C, U_{10} = 8\,ms^{-1}, q_s^* = 0.0274, Be = 0.248, R_H = 0.7$, and $\varphi = 1 \times 10^{-5}\,m^{-1}$. For the $C_{pw}/C_{pa} = 4$ curve, $C_{pw} = 4000 Jkg^{-1}K^{-1}$, and $C_{pa} = 1004 Jkg^{-1}K^{-1}$.

solution for both $\overline{P} = 0$ and $\overline{P} = \overline{E}$ cases are given in Appendix 1b (subsections i and ii). The solution, along with additional analytical analysis of this model, is also given in Behl (2012). For our hot spring parameters (Fig. 5) and $\overline{P} = 0$, $\rho_a \hat{Q}_a = 56.9\,kgs^{-1}$ and $\rho_w \hat{Q}_w = 6\,kgs^{-1}$, and for the $\overline{P} = \overline{E}$ case, $\rho_a \hat{Q}_a = 91.6\,kgs^{-1}$ and $\rho_w \hat{Q}_w = 6.4\,kgs^{-1}$. Simply put, the qualitative behavior of the hot spring model with moisture has all of key the features of the hot spring model without moisture.

d. Incompressible atmosphere–ocean model

The behavior of the incompressible atmosphere–ocean model is strikingly similar to both of our conceptual hot spring models (Sections 2a and 2b). Using our ocean parameters (see caption of Fig. 9), we find that and $\rho_a \hat{Q}_a = 2.67 \times 10^{10}\,kgs^{-1}$ and $\rho_w \hat{Q}_w = 10.5 \times 10^9\,kgs^{-1} (\hat{Q}_w = 10.5Sv)$. Within the asymptotic state, a large increase in $\rho_w Q_w$ causes only a small increase in $\rho_a Q_a$ (Fig. 9), a small increase in $(T_{ao} - T_{ai})$, a small decrease in $T_{wi} - T_{wo}$ (Fig. 10, upper left panel), and a small increase in both the latent heat flux and the sensible heat flux (Fig. 10, upper right panel; and Fig. 11).

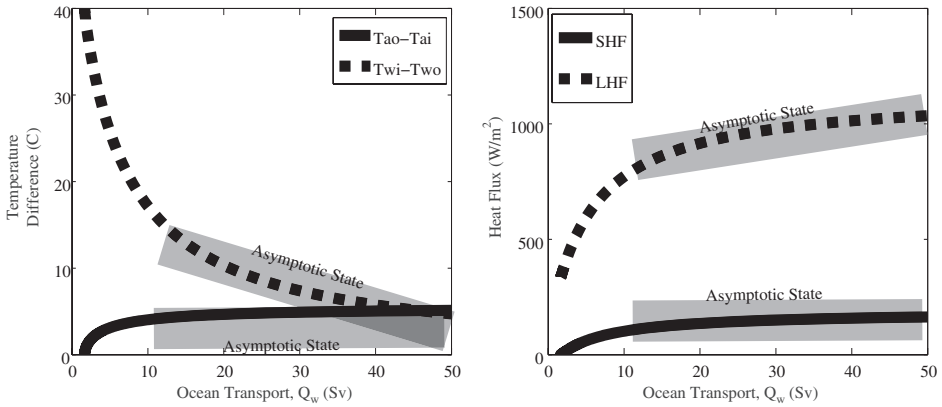

Figure 10. The temperature loss of the ocean and temperature gain of the atmosphere as a function of ocean transport Q_w (left panel); the mean sensible and latent heat fluxes as a function of the ocean transport (right panel) for $C_{pw}/C_{pa} = 4$ in the incompressible atmosphere–ocean model. Shading indicates the asymptotic state. LHF and SHF refer to the latent heat flux and sensible heat flux, respectively.

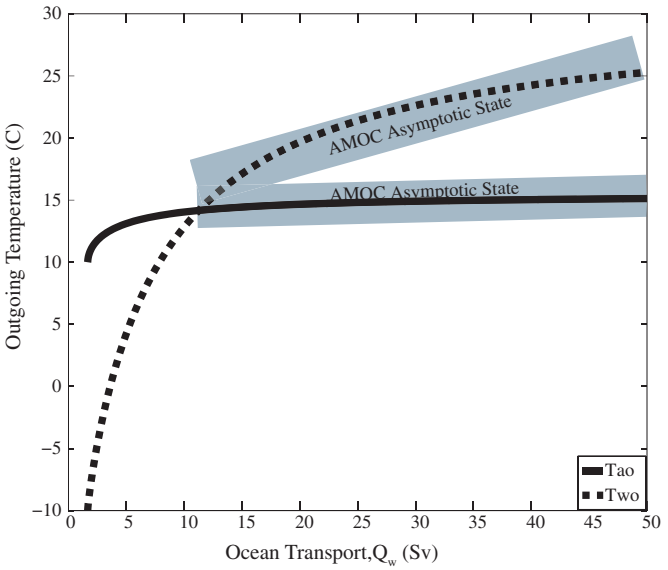

Figure 11. The outgoing atmospheric and oceanic temperatures as a function of the ocean transport, Q_w, for $C_{pw}/C_{pa} = 4$ in the incompressible atmosphere–ocean model. Within the asymptotic state, changes in the outgoing ocean temperature are larger than changes in the outgoing temperature of the atmosphere. In response to a reduction in the ocean transport, the ocean cools more than the atmosphere above it. There is a cutoff point on the left below which there are no (steady) solutions. At that point, the sensible heat flux is zero and the air is no longer being cooled ($T_{ao} = T_{ai}$). The shading indicates the asymptotic state.

From (Fig. 9 and [A33]), we see that the minimum value of Q_w at which atmospheric convection stops ($Q_a = 0$) is the same as in the hot spring model without moisture; $Q_{w_{\min}} = [A\rho_a c_L LeU_{10}q_S^*(1 - R_H)]/[2\rho_w C_{pw}(T_{wi} - T_{ai})]$. From (26) and (5), we see that $T_{ao} = T_{ai}$ and the mean sensible heat flux to the atmosphere is zero at $Q_w = Q_{w_{\min}}$.

We also looked at the sensitivity of the incompressible atmosphere–ocean model to the wind speed, the radius of convection region, and the temperature difference of the incoming water and air. Figure 12 shows that the asymptotic value $\rho_a \hat{Q}_a$ increases with an increase in any one of these three variables.

e. Compressible atmosphere–ocean model

The compressible model is our most realistic convection model, and yet, the results are surprisingly similar to those of the previous simpler models. An increase in the oceanic mass flux $\rho_w Q_w$ causes a nonlinear increase in the atmospheric mass flux $\rho_a Q_a$ (Fig. 14), decrease in temperature difference of the ocean, increase in temperature difference of the atmosphere (Fig. 15, upper left panel), and increase in the heat fluxes (Fig. 15, upper right panel). Using typical North Atlantic parameters (see caption of Fig. 14), we find that $\rho_a \hat{Q}_a = 3.08 \times 10^{10}\, kgs^{-1}$ and $\rho_w \hat{Q}_w = 10.6 \times 10^9\, kgs^{-1} (\hat{Q}_w = 10.6\ Sv)$. Note that this value is virtually identical to $\rho_w \hat{Q}_w$ in the incompressible atmosphere model. From (Fig. 14 and [A40]), we see that (as in all $\overline{P} = 0$ cases) atmospheric convection stops ($Q_a = 0$) at a positive value of the ocean transport,

$$Q_{w_{\min}} = [A\rho_a c_L LeU_{10}q_s^*(1 - R_H)]/[2\rho_w C_{pw}(T_{wi} - T_{ai})].$$

Based on our value for $\hat{Q}_w$ and its sensitivity to the parameters r_0, U_{10}, and $(T_{wi} - T_{ai})$ (Fig. 17), we estimate that 8–12 *Sv* marks the onset of the asymptotic state (for our compressible ocean–atmosphere model). As it turns out, this is the same as the estimate provided by the incompressible atmosphere–ocean model (see Appendix 1d, subsection ii), despite the differences in the two models. Lest the reader think that our ocean parameters were chosen so that the compressible and incompressible models would give identical results, there are significant differences in the other model variables. For example, the height D to which the air parcels rise is 1,934 m in the incompressible model but only 1,439 m in the compressible model.

The above result suggests that the AMOC, which is currently on the order of 20 *Sv*, may be in the asymptotic state, and, therefore, that a relatively large decrease in the AMOC transport would not produce a significant decrease in the temperature of the atmosphere or the sensible and latent heat fluxes from AMOC. From (A41), we see that the asymptotic value $\rho_a \hat{Q}_a$ depends on the area of the convection region, the incoming ocean–atmosphere temperature difference, and the wind speed. Figure 17 shows that $\rho_a \hat{Q}_a$ increases with an increase in any one of these three variables.

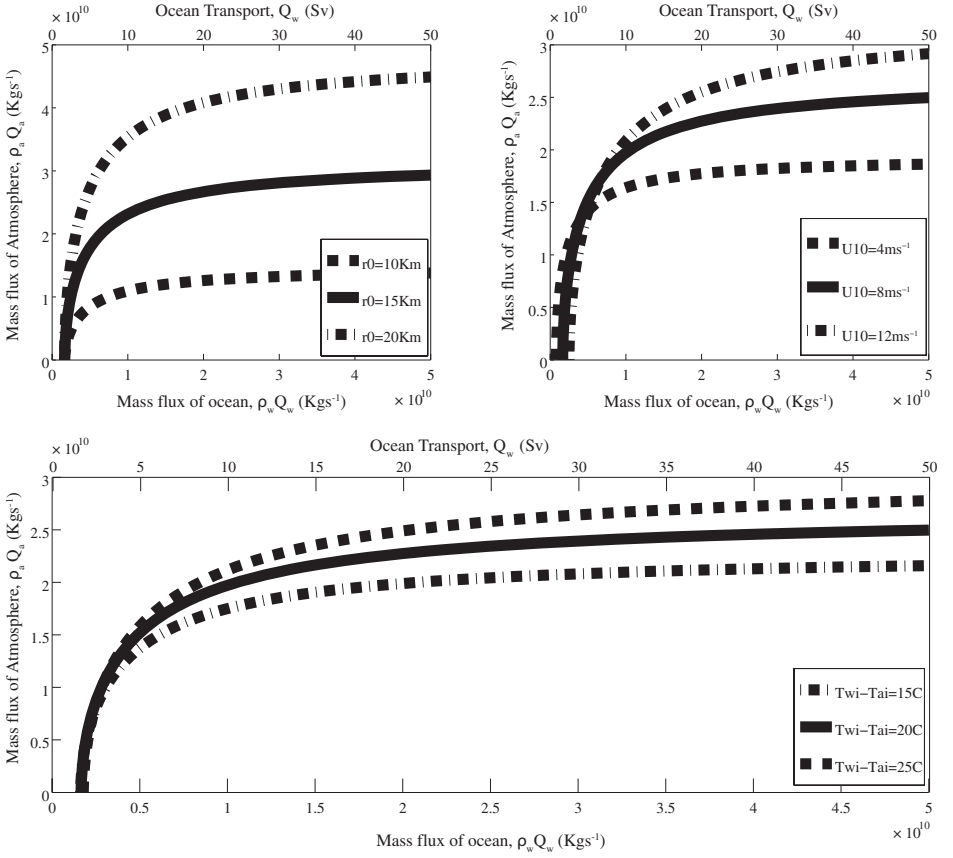

Figure 12. The atmospheric mass flux, $\rho_a Q_a$, versus the oceanic mass flux, $\rho_w Q_w$, for the incompressible atmosphere–ocean model with different convection zone radii (top left panel), different horizontal speeds (top right panel), and different temperature differences of the incoming water and air (bottom panel). Increasing any one of these parameters increases the asymptotic value $\rho_a \hat{Q}_a$. Smaller values of U_{10} reduce the asymptotic onset value $\rho_w \hat{Q}_w$, whereas for higher speeds, $\rho_w \hat{Q}_w$ is increased and the system moves away from asymptotic. The parameters r_0 and $(T_{wi} - T_{ai})$ have only a minimal effect on $\rho_w \hat{Q}_w$. The solid curves represent the North Atlantic. For all curves, the remaining parameters are held fixed at the values given in the caption of Figure 9.

4. Discussion and summary

We developed a series of four simple models with an increasing level of complexity (Fig. 2, Tables 1 and 2). Because of their extreme simplicity, such models cannot be satisfyingly applied to the ocean but, hopefully, imitate at least some aspects of the real atmosphere–ocean heat exchange process. Using bulk formulas for the air–sea surface fluxes and simple convection equations for the atmosphere, we examined the heat exchange between the

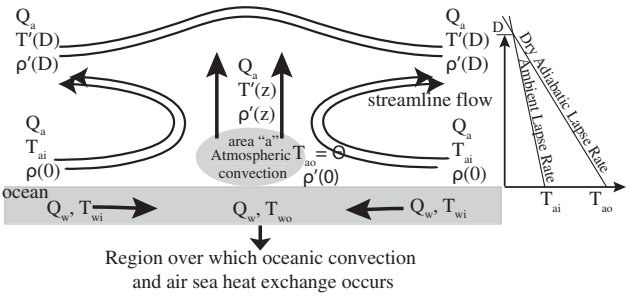

Figure 13. The compressible atmosphere–ocean model. A parcel in the small convection region (area $= a$) starts its rise from the surface at a warmer temperature than the surface ambient air but cools at a faster (dry adiabatic) rate than the ambient air as it rises. At the maximum height D, the density (and temperature) of the parcel match the density (and temperature) of the ambient air. The parameters $\rho(0)$ and T_{ai} are the density and temperature of the cold incoming surface air. The parameters $\rho'(0)$ and T_{ao} are the density and temperature of the heated parcel just before it starts its vertical rise. The parameter $\rho'(z)$ is the density, and $T'(z)$ is the temperature of the rising warm air parcel. The parameter $\rho'(D)$ is the density of the rising parcel when its temperature $T'(D)$ matches that of the ambient air at the equilibrium height D. The incoming and outgoing oceanic temperatures are T_{wi} and T_{wo}. The plot on the right-hand side of the figure shows the atmospheric vertical temperature profile in the environment (labeled T_{ai} at the surface) and in the convection region (labeled T_{ao} at the surface).

AMOC and the atmosphere, a process that at present is poorly understood. Our series of models cover a wide range of scales with very different physical configurations and underlying assumptions. The fact that the qualitative behavior of the small-scale hot spring models is the same as the large-scale atmosphere–ocean models provides evidence that all our models are good analogs for understanding some aspects of the large-scale atmosphere–ocean exchange and convection processes. In particular, all our models have a regime that we termed the "asymptotic state" (or "asymptotic regime"), suggesting that the asymptotic state concept is a robust feature (across a wide range of scales) of air–sea interactions that incorporate bulk-formula-based surface exchange processes and buoyancy-driven convection. The parameters in our models can be thought of as representative parameters for typical convection regions in the North Atlantic region. For example, the area of the convection region in our incompressible and compressible atmosphere–ocean models should be thought of as a total "effective" single area indicative of the aggregate of several smaller convection regions (1 km or so in diameter) over the entire North Atlantic region.

Before we begin a summary discussion of the asymptotic state and other important aspects of our models based on a description of model results, we should stop and examine the basic physics underlying the existence of the asymptotic state. Many readers may in fact be wondering why should there even be an asymptotic state in the first place. To be precise, why should all the dependent variables that describe the modeled atmosphere–ocean system asymptote to a fixed maximum value as the independent variable Q_w becomes large?

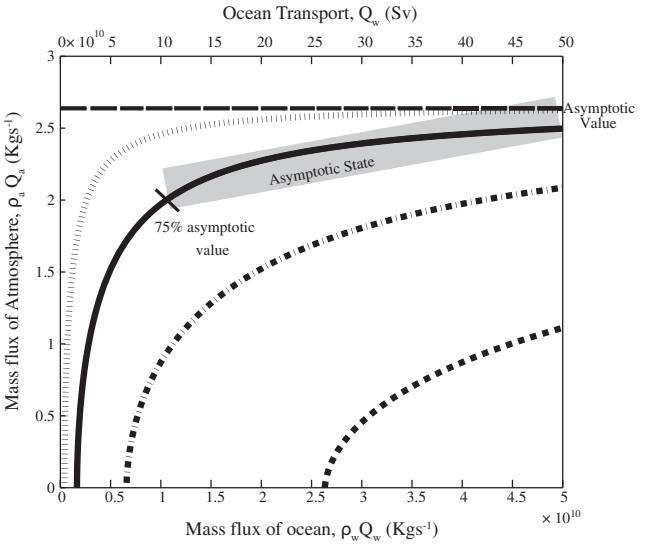

Figure 14. The atmospheric mass flux, $\rho_a Q_a$, versus oceanic mass flux, $\rho_w Q_w$, for various hypothetical values of C_{pw}/C_{pa} (with C_{pa} fixed) in the compressible atmosphere–ocean model. As before, the specific heat capacities only control the onset of the asymptotic state $\rho_w \hat{Q}_w$, which occurs at lower values of $\rho_w Q_w$ for higher values of C_{pw}/C_{pa}. The parameters are $r_0 = 17.2\,km$, $r_1 = 500\,km$, $c_S = 0.0009$, $c_L = 0.00135$, $\rho_a = 1.5\,kgm^{-3}$, $\rho_w = 1,000\,kgm^{-3}$, $Le = 2.5 \times 10^6 Jkg^{-1}$, $g = 9.8\,ms^{-2}$, $T_{ai} = 10°C$, $T_{wi} = 30°C$, $U_{10} = 8\,ms^{-1}$, $q_s^* = 0.0274$, $Be = 0.248$, $R_H = 0.7$, $\gamma_D = 0.00980°\,km^{-1}$, and $\gamma = 0.00649°km^{-1}$. Note that parameters that are common to the incompressible and compressible atmosphere–ocean models have the same value in both models.

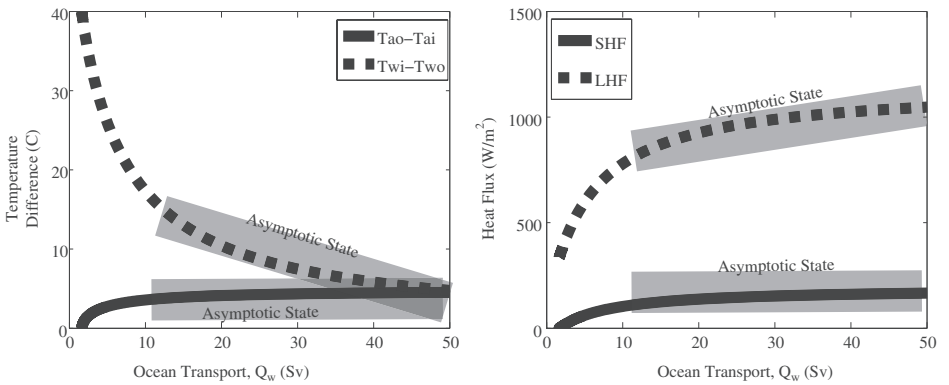

Figure 15. The ocean temperature loss and the air temperature gain as a function of ocean transport, Q_w (left panel); the mean sensible and latent heat fluxes as a function of ocean transport (right panel) for $C_{pw}/C_{pa} = 4$ in the compressible atmosphere model. Shading indicates the asymptotic state. LHF and SHF refer to the latent heat flux and sensible heat flux, respectively.

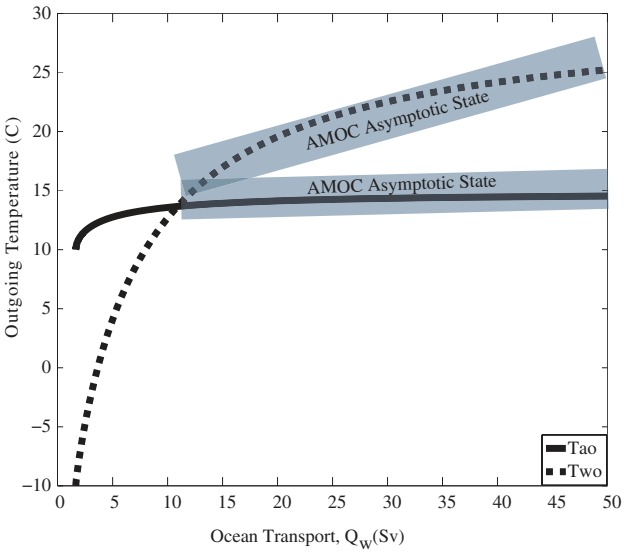

Figure 16. Outgoing atmospheric and oceanic temperatures as a function of ocean transport, Q_w, for $C_{pw}/C_{pa} = 4$ in the compressible atmosphere–ocean model. Within the asymptotic state, changes in the outgoing ocean temperature are larger than the changes in the outgoing atmospheric temperature. In response to a reduction in the oceanic transport, the ocean cools much more than the atmosphere above it. As before, there is a cutoff point below which there are no (steady) solutions. At that point the sensible heat flux is zero and the air is no longer being cooled ($T_{ao} = T_{ai}$). The shading indicates the asymptotic state.

Concisely stated, the physical reason for asymptotic state is that while in the atmosphere an increase in heat flux (to the atmosphere) is associated with both an increase in the atmospheric transport and an increased warming of the air $[(T_{ao} - T_{ai}) > 0]$, in the ocean, an increase in the heat flux (from the ocean) is associated with a decreased cooling of the water $[(T_{wi} - T_{wo}) < 0]$ and a compensating increase in the ocean transport.

With an increase in heat flux, there is decrease in the temperature loss of the ocean (ocean is being cooled) and an increase in the temperature gain of the atmosphere (atmosphere is being warmed). The (warmer) ocean cools less than the (cooler) air above it, resulting in an increase in the temperature difference between the ocean and the atmosphere. When the mean temperature difference between the ocean and the atmosphere is the greatest, the atmospheric transport Q_a approaches its maximum "asymptotic" value, and the compensating ocean transport increases to infinity.

To more clearly understand this, we will consider our model equations in a more qualitative manner. The fact that a heat flux to the atmosphere warms the air ($T_{ao} > T_{ai}$) and a heat flux from the ocean cools the water ($T_{wo} < T_{wi}$) is both intuitively obvious and correct,

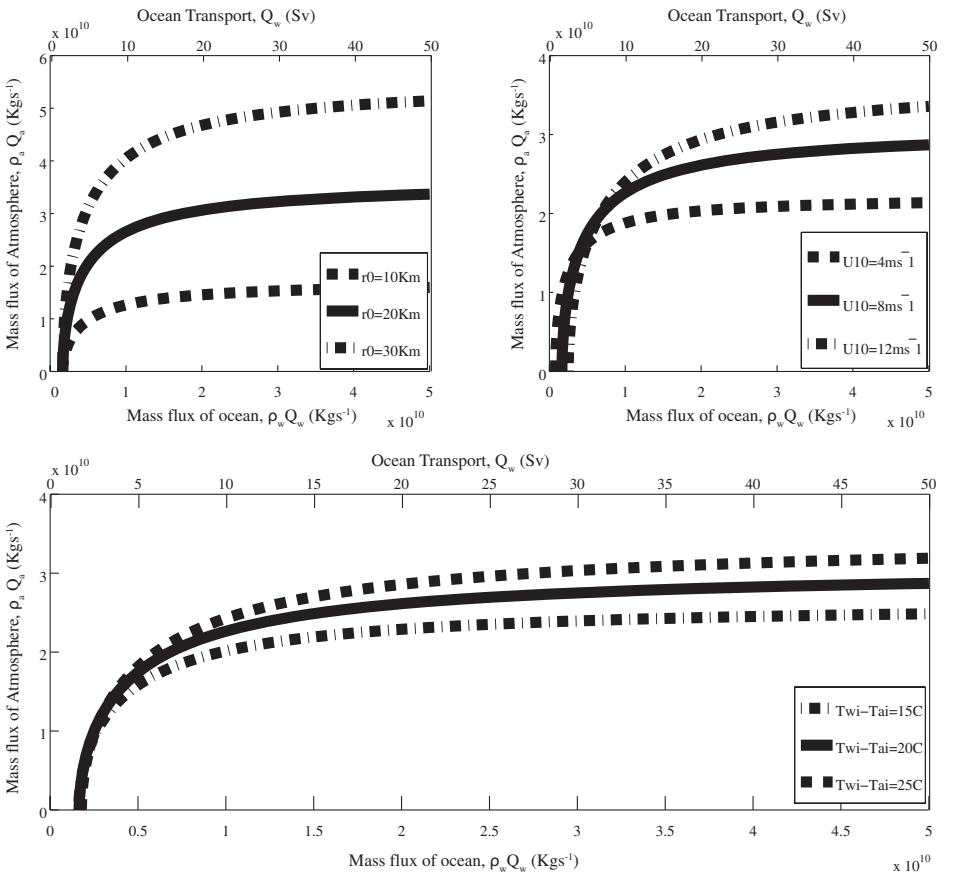

Figure 17. The atmospheric mass flux, $\rho_a Q_a$, versus oceanic mass flux, $\rho_w Q_w$, for the compressible atmosphere model using different radii of convection region (top left panel), different horizontal speeds (top right panel), and different temperature differences of the incoming water and air (bottom panel). Increasing any one of these parameters increases the asymptotic value $\rho_a \hat{Q}_a$. Smaller values of U_{10} reduce the asymptotic onset value $\rho_w \hat{Q}_w$, whereas for higher speeds, $\rho_w \hat{Q}_w$ is increased and the system departs from asymptotic. The parameters r_0 and $(T_{wi} - T_{ai})$ have only a minimal effect on $\rho_w \hat{Q}_w$. The solid curves represent conditions similar to those in the North Atlantic. For all curves, the remaining parameters are held fixed (the values given in the caption of Fig. 14).

but understanding what happens when we change the heat flux is not quite so simple and requires more careful consideration.

For most of our models and, again, for the sake of the physical argument here, the atmospheric transport Q_a increases with the "heating" (temperature gain) of the atmosphere $(T_{ao} - T_{ai})$, which is an intuitively appealing property. (See the bottom row of Tables 1 and 2 for a summary of the atmospheric transport equations.) Both the transport and Q_a the

temperature gain ($T_{ao} - T_{ai}$) in the product on the Left-Hand-Side (LHS) of the atmospheric heat equation increase as a result of an increase in the heat flux to the atmosphere. Because the atmosphere is warmed, and because the ocean is warmer than the atmosphere, an increase in the heat flux to the atmosphere, which is associated with an increase in the mean ocean–atmosphere temperature difference, requires an (even larger) increase in the mean ocean temperature. The surprising and counterintuitive result is that the ocean is being cooled less (compared with the air above it) despite the fact that the heat flux from the ocean has increased. Because the heat flux from the ocean (on the RHS of atmospheric heat equation) has increased, the ocean transport Q_w must increase strongly to overcome the decrease in the ocean cooling. Because there is relatively more water to be cooled, therefore, the cooling of the ocean is reduced and the mean and outgoing ocean temperatures rise.

Summarizing all this, we would say that as the atmospheric transport Q_a, the air temperature gain ($T_{ao} - T_{ai}$), the heat flux to the atmosphere, the heat flux from the ocean, the mean air temperature, the mean water temperature, and the mean ocean–atmosphere temperature difference all continue to increase together, they all reach their finite maximum "asymptotic" values (as the outgoing ocean temperature T_{wo} increases to T_{wi}). In the (complete) asymptotic state, the finite heat flux from the ocean does not cool the infinite ocean transport, but the finite heat flux to the atmosphere does warm the finite atmospheric transport. It is worthwhile to reiterate here that each of the properties (1) to (3) in the Abstract is a prerequisite for the physics discussed above to hold, and that without property (4), the present-day AMOC would likely not be in the asymptotic state, because the onset value would be too high. We now continue with a discussion of our model results.

a. The asymptotic state

The most important result is the existence of a dynamic asymptotic state. In that regime, changes in the AMOC transport have very little effect on the outgoing atmospheric temperature. The mass-flux of the atmosphere $\rho_a \hat{Q}_a$ decreases with a decrease in AMOC transport. We define the onset of the asymptotic state as the value of the ocean transport (ocean mass flux), where the atmospheric mass flux $\rho_a Q_a$ reaches 75% of its maximum asymptotic value $\rho_a \hat{Q}_a$. Within the asymptotic state, even a large reduction (e.g., 50%) of the AMOC does not result in a significant reduction of the atmospheric mass flux. Because the atmospheric mass flux does not change much, the associated changes in the ocean and atmospheric temperatures, and the latent and sensible heat fluxes, are also small. Using typical values for the North Atlantic with the most realistic (compressible) atmosphere–ocean convection model, we estimate the lower limit transition to the asymptotic state to occur when the AMOC transport is 8–12 *Sv*. This suggests that, in reality, the variability of the AMOC may not be as important as the conventional wisdom suggests. The relatively warm ocean cools less than the cool air above it, resulting in a small reduction in the air–sea temperature difference. This small reduction in the air–sea temperature difference is associated with the small decrease in the heat fluxes discussed above.

A very dramatic reduction in the conceptual AMOC transport (e.g., 500%) leads the system to move out of the asymptotic state. Once outside the asymptotic state, the system behaves as one normally would expect (i.e., even a small reduction in the AMOC transport would cause a large decrease in the atmospheric transport). This large decrease in atmospheric transport causes a large decrease in both the ocean and atmospheric temperatures and the heat fluxes. This situation is in line with common ideas, and with the occurrence of Heinrich events, but we suggest that it is not relevant to the present-day AMOC. In general, our models agree with the global numerical models that the atmosphere in the northern Atlantic region would cool as a result of a decrease in the strength of the AMOC. However, in contrast to the global numerical model results, we find that this atmospheric cooling would be insignificant because the present-day AMOC system is in its asymptotic regime.

At this stage, it is impossible to say what processes in the numerical models are responsible for this disagreement. Although a resolution of this issue is very important, it is so involved that it would be a project on its own right and is, therefore, left as a subject for future investigation by numerical modelers, observationalists, as well as theoreticians. One possible candidate for the discrepancy is sea ice, which is increased by the hosing that is typically used to numerically examine a reduction in the AMOC. Sea ice increases the radiation back to space, cooling the atmosphere through a mechanism unrelated to the AMOC. A change in North Atlantic storm tracks is another possibility. The reader who wonders about the neglect of radiation in the open-ocean, "no-roof" models is referred to Nof, Van Gorder, and Yu (2011), who have argued that radiation is probably not important to the variability of the AMOC.

b. Factors affecting asymptotic state

For the case in which the atmosphere gains only sensible heat (i.e., no rain within the limits of the ocean, $\overline{P} = 0$) the maximum asymptotic value $\rho_a \hat{Q}_a$ is independent of both C_{pw} and C_{pa}. The specific heat capacities control the onset value of the asymptotic state, but not the limiting asymptotic value $\rho_a \hat{Q}_a$. This can be seen in Figures 5, 9, and 14 showing the results for the hot spring model without moisture, the incompressible atmosphere–ocean model, and the compressible atmosphere–ocean model. For the case in which the atmosphere gains both the latent and sensible heat (i.e., whatever evaporates rains back over the ocean within the interaction region of interest, $\overline{P} = \overline{E}$), the maximum asymptotic value $\rho_a \hat{Q}_a$ depends only on C_{pa}. However, as in the $\overline{P} = 0$ case, both C_{pa} and C_{pw} control the onset value of the asymptotic state. We see in Figures 5, 9, and 14 that higher values of C_{pw} are associated with lower asymptotic onset values, illustrating the point that the asymptotic state owes its existence (i.e., the existence of a reasonably low asymptotic onset value) to the relatively high specific heat capacity of water compared with air. In the hypothetical limit $C_{pw} \to \infty$, $\rho_w \hat{Q}_w$ tends to zero and the system becomes completely asymptotic, with no change in the atmospheric response regardless of the change in $\rho_w Q_w$. Of course, the fact that the ocean is warmer than the atmosphere, that atmospheric convection increases

with the heating of the atmosphere, and that the heat flux is generally "proportional" to the ocean–atmosphere temperature difference are also key prerequisites for the physics underlying the existence of the asymptotic state (as described above) to hold.

We also examined the sensitivity of our incompressible (Fig. 12) and compressible (Fig. 17) atmosphere–ocean models to variations in the wind speed U_{10}, the radius of the convection region r_0, and the incoming temperature difference of the ocean and the atmosphere $(T_{wi} - T_{ai})$. As seen in Figures 12 and 17, increasing any one of these parameters increases the asymptotic value $\rho_a \hat{Q}_a$. Smaller values of U_{10} reduce the asymptotic onset value $\rho_w \hat{Q}_w$, thus expanding the domain of the asymptotic state, whereas r_0 and $(T_{wi} - T_{ai})$ have only a minimal effect on $\rho_w \hat{Q}_w$.

Why is there no solution for weak ocean transport in Figures 5, 9, and 14? This is because of the no-precipitation assumption in both the incompressible and compressible atmosphere–ocean models and, of course, in the $\overline{P} = 0$ of the hot spring model without moisture. As previously noted, for all three models there is a finite value of the ocean transport,

$$Q_{w_{\min}} = [A\rho_a c_L Le U_{10} q_s^*(1 - R_H)]/[2\rho_w C_{pw}(T_{wi} - T_{ai})].$$

at which the atmospheric transport Q_a goes to zero and the atmosphere is not being heated (i.e., $T_{ao} = T_{ai}$ and $\overline{F}_s = 0$). As is shown in Figures 5, 9, and 14, a plot of Q_a as a function of Q_w does not pass through the origin. For values of Q_w smaller than $Q_{w_{\min}}$, Q_a, would become negative and the atmosphere would be cooled by the ocean, which is not allowed. Because of the no-precipitation assumption, the atmosphere is heated only by sensible heat (5), whereas the ocean is cooled by both latent and sensible heat (6). If the heat added to the atmosphere were equal to the heat removed from the ocean, as in the $\overline{P} = \overline{E}$ case, then the plot of Q_a as a function of Q_w would have passed through the origin as shown by (10). Thus, for $\overline{P} = \overline{E}$ cases (which only applies to the hot spring models), we do have weak ocean transport solutions.

c. Model weaknesses

Like all simple models, the models presented here have substantial weaknesses, the most important of which is probably the neglect of preexisting zonal atmospheric flows, which, in addition to the free atmospheric convection discussed here, absorb some of the heat released by the ocean. We have only included some effects of mean wind by choosing the value of U_{10} in the heat flux bulk formulas to reflect typical values ($U_{10} \sim 1.35$ m s^{-1} for hot spring models, $U_{10} \sim 8$ m s^{-1} for incompressible and compressible atmosphere–ocean convection models). The surface wind induced by convection in our models is small compared with our choice of U_{10}. The neglect of preexisting zonal atmospheric flows may be one reason for disagreement between the results of our models and numerical model results. The second potentially important weakness is the neglect of rotation. Although the convection itself is fast (minutes) so that rotation probably does not affect it directly, the

horizontal atmospheric flows into and out of the convection region (i.e., at the bottom and top of the two open-ocean models) probably occur through Ekman layers, which have been neglected here. It is hard to anticipate what the effect of these Ekman layers would be, but their effect is expected to be important. Another important weakness is that in the actual ocean, the cooling does not only occur over the convection region itself but rather over both the Gulf Stream as it progresses northward and the convection region. For tractability, we have lumped both of these regions into one chamber. Because the models involve gradients in two directions (horizontal and vertical), one can say that our model is two-dimensional, whereas the real system is three-dimensional. This is no doubt a weakness, but not one of critical importance. One last potential weakness of our study is that, even though the temperature of water changes from T_{wi} to T_{wo}, the incoming water temperature T_{wi} is held at a fixed value. This assumption makes the algebra easy but prevents easy comparison with the numerical models. In numerical models, the subtropical upper water temperature fields vary with the strength of the AMOC. When the AMOC reduces, then there is cooling in the North Atlantic, including the subtropics, and when it strengthens, there is surface warming (Knight et al. 2005).

To summarize, we found that the simplified atmosphere (and the ocean) can only cool in response to a reduction in the AMOC mass transport. We showed that for both of our open-ocean models, the AMOC system is in an asymptotic state when the ocean transport exceeds 8–12 *Sv*. In this regime, the atmospheric cooling caused by a reduction in the AMOC is very small. We see in Figures 9 and 14 that a reduction of the AMOC transport from 20 to 10 *Sv* results in a ∼15% reduction in the mass flux of the atmosphere, and, from Figures 11 and 16, we see about a 1 degree reduction in T_{ao}. Whether this is quantitatively an important impact is not really the point. The point of these models is to show that the asymptotic regime exists, and that if either the AMOCs was smaller than its present-day value, or the ratio C_{pw}/C_{pa} was smaller than 4, then the reduction in atmospheric temperatures would be much more severe.

Acknowledgments. This work was supported by National Science Foundation grants (OCE-0752225, OCE-0928271, OCE-0545204, ARC-0902835, and ARC-0453846). D. Nof thanks Yochanan Kushnir for his valuable input regarding the sea-ice issue.

APPENDIX 1

a. Hot spring model without moisture

i. Solution for $\overline{P} = 0$. As mentioned, for tractability, we take the volume flux of the air Q_a (instead of the water flux) as known and solve the three equations (4), (5), and (6) for the unknowns T_{ao}, T_{wo}, and Q_w. To begin, we determine the outgoing air temperature T_{ao} from (4) as follows:

$$T_{ao} = T_{ai} + (1/2gD\alpha)(Q_a/a)^2. \tag{A1}$$

We then substitute (A1) into (5) to solve for T_{wo} as follows:

$$T_{wo} = T_{wi} + (1/2gD\alpha)(Q_a/a)^2\{(2Q_a/Ac_SU_{10}) + 1\} - 2(T_{wi} - T_{ai}). \tag{A2}$$

Finally, we substitute (A1) and (A2) into (6) to solve for Q_w as follows:

$$\begin{aligned} Q_w = {} & \frac{(Q_a^3/c_S)(\rho_a C_{pa}/\rho_w C_{pw})(c_S + c_L R_H/Be)}{2gD\alpha a^2[2(T_{wi} - T_{ai}) - (Q_a^2/2gD\alpha a^2)\{(2Q_a/Ac_SU_{10}) + 1\}]} \\ & + \frac{A\rho_a c_L LeU_{10}q_s^*(1 - R_H)}{\rho_w C_{pw}[2(T_{wi} - T_{ai}) - (Q_a^2/2gD\alpha a^2)\{(2Q_a/Ac_SU_{10}) + 1\}]}. \end{aligned} \tag{A3}$$

A few important conclusions can immediately be drawn from (A2) and (A3). For $T_{wo} < T_{wi}$ and positive Q_a, the volume flux Q_w is also positive. $Q_w \to \infty$ as $(T_{wi} - T_{wo}) \to 0$; that is, as $Q_w \to \infty$, $T_{wo} \to T_{wi}$, and Q_a tends to finite value $\hat{Q}_a$. The relationship between Q_a and Q_w depends on both C_{pw} and the specific heat capacity ratio C_{pa}/C_{pw}. There is clearly a nonlinear relationship between Q_a and Q_w, and atmospheric convection stops ($Q_a = 0$) at a positive value of Q_w.

ii. Nondimensional analysis of the hot spring model without moisture, $\overline{P} = 0$ case. First, we nondimensionalize using the following:

$$Q_a^* = Q_a/a(2gD)^{1/2},\ Q_w^* = Q_w/a(2gD)^{1/2},\ T_a^* = \alpha(T_{ao} - T_{ai}),\ T_w^* = \alpha(T_{wi} - T_{wo}),$$
$$\Delta T^* = \alpha(T_{wi} - T_{ai}),\ C_{pw}^* = (C_{pw}/\alpha Le),\ C_{pa}^* = (C_{pa}/\alpha Le),\ c_L^* = (Ac_LU_{10})/\{2a(2gD)^{1/2}\},$$
$$c_S^* = (Ac_SU_{10})/\{2a(2gD)^{1/2}\}.$$

All of the above parameters are positive (the cooler atmosphere gains heat and is warmed while the warmer ocean loses heat and is cooled). Using these definitions, the nondimensional solutions T_a^*, T_w^*, and Q_w^*, in terms of Q_a^*, are

$$T_a^* = (Q_a^*)^2, \tag{A4}$$

$$T_w^* = 2\Delta T^* - \{(Q_a^*/c_S^*) + 1\}(Q_a^*)^2, \tag{A5}$$

$$Q_w^* = \frac{[(Q_a^{*3}/c_S^*)(\rho_a C_{pa}^*/\rho_w C_{pw}^*)(c_S^* + c_L^* R_H/Be)]}{[2\Delta T^* - Q_a^{*2}\{(Q_a^*/c_S^*) + 1\}]} + \frac{[2(\rho_a C_L^*/\rho_w C_{pw}^*)\{q_s^*(1 - R_H)\}]}{[2\Delta T^* - Q_a^{*2}\{(Q_a^*/c_S^*) + 1\}]}. \tag{A6}$$

As mentioned, Q_a^* is temporarily taken to be known. From (A4), one can see that T_a^* is positive and decreases with decreasing Q_a^*; that is, the air temperature gain $(T_{ao} - T_{ai})$ decreases with a decrease in the airflow through the bathhouse Q_a. Similarly, from (A5), we conclude that T_w^* and $T_{wo} - T_{wi}$ are always positive (i.e., the hot water always loses heat and is cooled) as long as $[\{(Q_a^*/c_S^*) + 1\}Q_a^{*2}] < 2\Delta T^*$, and that T_w^*, the water temperature loss, increases with a decrease in Q_a^*.

Five important conclusions can be drawn from a close examination of (A4), (A5), and (A6).

1. Nonlinear dependence of Q_a^* on Q_w^*: For positive T_w^*, Q_w^*, is positive and decreases with a decrease in Q_a^*. Thus, T_a^* and Q_w^* decrease, and T_w^* increases with a decrease in Q_a^*. The corollary is also true; that is, a decrease in Q_w^* results in a nonlinear decrease in Q_a^* (Fig. 5). Thus, the variables Q_a^* and T_a^* decrease, and T_w^* increases with a decrease in Q_w^*; that is, the atmospheric transport decreases, and both the hot spring water and the air cool with a reduction in water mass flux. From (A6), one can also conclude that Q_w^* has a positive value when $Q_a^* \to 0$ (Fig. 5). At that point, we see from (A4) that $T_{ao} - T_{ai}$ and from (5) of the main text that both the mean sensible heat flux and the mean air water temperature difference are zero. Although the air is no longer being warmed, the water is still being cooled by the part of the latent heat flux that does not depend on the temperature difference. For $0 < Q_w^* < [\rho_a c_L^* q_S^*(1 - R_H)/\rho_w C_{pw}^* \Delta T^*]$, there are no steady solutions.

2. Cooling rate of the air and water and changes in the heat flux: Differentiating (A4) and (A5) with respect to Q_a^* gives

$$dT_a^*/dQ_a^* = 2Q_a^*, \tag{A7}$$

$$-dT_w^*/dQ_a^* = (Q_a^{*2}/c_S^*) + 2Q_a^*\{1 + (Q_a^*/c_S^*)\}. \tag{A8}$$

Comparing (A7) and (A8), we arrive at

$$-dT_w^*/dQ_a^* > dT_a^*/dQ_a^*,$$

which implies

$$-dT_w^*/dQ_w^* > dT_a^*/dQ_w^* > 0 \text{ because } dQ_w^*/dQ_a^* > 0. \tag{A9}$$

Equation (A9) shows that, with decreasing Q_w^*, both the air and the water cool. In addition, (A9) shows that with decreasing Q_w^*, the (warmer) water in the hot spring cools faster than the (cooler) air above it, decreasing the water-air temperature difference and, therefore, reducing the sensible and latent heat fluxes. We summarize by saying that with a reduction of the hot spring water transport, the air transport decreases resulting in an increase in the water temperature loss ($T_{wi} - T_{wo}$) and a decrease the air temperature gain ($T_{ao} - T_{ai}$) (Fig. 6, upper left panel). The (warmer) water cools more than the (cooler) air above it (Fig. 7), and the resultant decrease in the temperature difference between the water and the air results in a decrease in both the sensible and latent heat flux from the ocean and a decrease in the sensible heat flux to the atmosphere (Fig. 6, upper right panel).

3. Asymptotic value of Q_a^*: From (A5) and the requirement that $T_w^* > 0$, we see that Q_a^* increases from zero, T_w^* decreases from $2\Delta T^*$ and becomes zero at some value $\hat{Q}_a^*$, which is the maximum allowed value of Q_a^*. At $Q_a^* = \hat{Q}_a^*$, the water can no longer be cooled as it passes through the hot spring because, according to (A6), Q_w^* has become infinite. For $Q_a^* > \hat{Q}_a^*$, (A6) implies that the requirement $Q_w^* > 0$ is violated. When Q_a^* is viewed as a function of Q_w^*, we see that Q_a^* asymptotes to $\hat{Q}_a^*$ as $Q_w^* \to \infty$ (Fig. 5).

Setting $T_w^* = 0$ in (A5) yields a cubic equation for $\hat{Q}_a^*$, $\hat{Q}_a^{*3} + c_S^* \hat{Q}_a^{*2} - 2c_S^* \Delta T^* = 0$.

Neglecting the second (quadratic) term (whose relationship to the first term is defined to be ε) yields the approximate solution

$$\hat{Q}_a^* \simeq (2c_S^* \Delta T^*)^{1/3}, \tag{A10}$$

which is valid for $\varepsilon = \{c_S^{*2}/(2\Delta T^*)\}^{1/3} = [(Ac_S U_{10})^2/\{16a^2 g D\alpha(T_{wi} - T_{ai})\}]^{1/3} \ll 1$. In dimensional form, (A10) becomes

$$\hat{Q}_a = \{2gDa^2 AU_{10}\alpha c_S(T_{wi} - T_{ai})\}^{1/3}. \tag{A11}$$

For the hot spring model parameters (see caption of Fig. 5), $\varepsilon \simeq 0.0007$, the exact "asymptotic" value for the mass flux of the air is 52.8 kg s^{-1}, and (A11) gives $\hat{Q}_a \simeq 55.1\, kg\ s^{-1}$.

4. The asymptotic state: The asymptotic behavior of Q_a for large Q_w is the principal characteristic of the regime that we have referred to as the "asymptotic state." We define the lower boundary or onset value of the asymptotic state as the value of $\hat{Q}_w$ where Q_a reaches 75% of its asymptotic value $\hat{Q}_a$. When the mass flux of the water exceeds $\rho_w \hat{Q}_w$, we say that the system is in the asymptotic state and all variables are only weakly sensitive to changes in the water mass flux.

We now go back to the mathematical problem (Q_a known and Q_w unknown) and derive an expression for $\hat{Q}_w^*$ by substituting $Q_a^* = \delta \hat{Q}_a^*$ into (A6), where δ is the asymptotic state threshold value, which we choose to be 0.75. Using our approximate solution for $\hat{Q}_a^*$ (A10), and ignoring terms that are quadratic in $\hat{Q}_a^*$ in the expression for T_w^* (A5), which appears in the denominator of both terms on the Righ-Hand-Side (RHS) of (A6), we obtain

$$\begin{aligned}\hat{Q}_w^* = {} & (\rho_a C_{pa}^*/\rho_w C_{pw}^*)(c_S^* + c_L^* R_H/Be)\{\delta^3/(1-\delta^3)\} \\ & + 2\rho_a c_L^* q_S^*(1 - R_H)/[\rho_w C_{pw}^*(2\Delta T^*)(1-\delta^3)].\end{aligned} \tag{A12}$$

In the dimensional form, (A12) is

$$\hat{Q}_w = (AU_{10}/2)(\rho_a/\rho_w)\left[\frac{(c_{pa}/c_{pw})(c_S + c_L R_H/Be)\delta^3}{(1-\delta^3)} + \frac{(c_L Le/C_{pw})\{q_s^*(1-R_H)\}}{\{(T_{wi} - T_{ai})(1-\delta^3)\}}\right]. \tag{A13}$$

For our hot spring parameters (see caption of Fig. 5) and our choice of $\delta = 0.75$, (A13) gives $\rho_w \hat{Q}_w \simeq 10.3\, kgs^{-1}$, very close to the exact value 9.9 $kg\ s^{-1}$. Note that (in Fig. 5) $\rho_w \hat{Q}_w$ is roughly at the point where the slope $(\rho_a/\rho_w)(dQ_a/dQ_w) = 1$, which was our original motivation for choosing $\delta = 0.75$.

5. Dependence of the asymptotic value $\hat{Q}_a$ and the asymptotic onset value $\hat{Q}_w$, on the heat capacities C_{pa} and C_{pw}: From (A11), we see that the asymptotic value of the air volume transport $\hat{Q}_a$, is *not* dependent on either the heat capacity of air or the heat capacity of water. On the other hand, (A13) shows that the asymptotic onset value $\hat{Q}_w$ depends on both the ratio (C_{pa}/C_{pw}) and $C_{pw} \cdot \hat{Q}_w$ decreases to a nonzero value as $C_{pa} \to 0$, but as

$C_{pw} \to \infty$, $\hat{Q}_w \to 0$ for all δ. In other words, in the hypothetical limit, $C_{pw} \to \infty$ (even for δ near 1), the asymptotic onset value, marking the lower boundary of the asymptotic state, decreases to zero. This means that, from this point and on, there can be no change in any of the variables Q_a, T_{ao}, T_{wo}, regardless of the change in Q_w.

iii. The $\overline{P} = \overline{E}$ case for hot spring model without moisture. Our equations are (4), (9), and (10), which we again, for mathematical simplicity, solve for T_{ao}, T_{wo}, and Q_w in terms of Q_a. As in the $\overline{P} = 0$ case, the solution for the temperature of the outgoing air T_{ao} is given by (A1). Substituting (A1) into (9) to obtain a solution for the temperature of the outgoing water T_{wo}, we find that

$$T_{wo} = T_{wi} + \left(\frac{Q_a^2}{2gD\alpha a^2}\right)\left[\left\{\frac{2Q_a}{AU_{10}(c_S + c_L R_H/Be)}\right\} + 1\right] \tag{A14}$$

$$- \frac{2c_L Leq_s^*(1 - R_H)}{\{C_{pa}(c_S + c_L R_H/Be)\}} - 2(T_{wi} - T_{ai}). \tag{A15}$$

Equations (10) and (A1) give

$$\begin{aligned} Q_w &= (\rho_a C_{pa}/\rho_w C_{pw}) Q_a (T_{ao} - T_{ai})/(T_{wi} - T_{wo}) \\ &= (\rho_a C_{pa}/\rho_w C_{pw}) Q_a^3/[\{2gD\alpha a^2\}(T_{wi} - T_{wo})], \end{aligned} \tag{A16}$$

where $(T_{wi} - T_{wo})$ is given by (A14).

The qualitative results for the case $\overline{P} = \overline{E}$ are similar to those for $\overline{P} = 0$, but some of the details are different. From (A15) and (A14), we will again find that the mass flux of the air decreases nonlinearly with a decrease in mass flux of the water and that the system has an asymptotic state. Note that, in contrast to the $\overline{P} = 0$ case, $Q_a = 0$ when $Q_w = 0$ (rather than at some positive value of Q_w), so there are steady physical solutions for all $Q_w > 0$.

In a similar manner to the $\overline{P} = 0$ case, the asymptotic value for Q_a is obtained by setting $(T_{wi} - T_{wo}) = 0$ and $Q_w \to \infty$ in (A14) and (A15). In the nondimensional form, (A14) is

$$\begin{aligned} T_w^* = {} & \{Q_a^{*3}/(C_S^* + c_L^* R_H/Be)\} + Q_a^{*2} \\ & - [2\Delta T^* + \{2c_L^* q_s^*(1 - R_H)/C_{pa}^*(c_S^* + c_L^* R_H/Be)\}]. \end{aligned} \tag{A17}$$

Setting $T_w^* = 0$ yields a cubic equation for $\hat{Q}_a^*$, $\hat{Q}_a^{*3} + k_2 \hat{Q}_a^{*2} + k_3 = 0$, where

$$\begin{aligned} k_2 &= (c_S^* + c_L^* R_H/Be) \\ k_3 &= -[2\Delta T^*(c_S^* + c_L^* R_H/Be) + \{2c_L^* q_s^*(1 - R_H)/C_{pa}^*\}]. \end{aligned}$$

Neglecting again the small quadratic term yields the approximate solution

$$\hat{Q}_a^* \simeq [2\Delta T^*\{c_S^* + c_L^* R_H/Be\} + 2c_L^* q_s^*(1 - R_H)/C_{pa}^*]^{1/3}, \tag{A18}$$

which is valid for $\varepsilon = [(c_S^* + c_L^* R_H/Be)^2/\{2\Delta T^* + 2c_L^* q_s^*(1 - R_H)/C_{pa}^*(c_S^* + c_L^* R_H/Be)\}]^{1/3} \ll 1$.

In a dimensional form,

$$\varepsilon = [\{(AU_{10})^2(C_S + C_L R_H/Be)^2\}/(16a^2 g D\alpha)\{(T_{wi} - T_{ai}) + C_L Leq_s^*(1 - R_H)/C_{pa}(C_S + C_L R_H/Be)\}]^{1/3},$$

and (A17) becomes

$$\hat{Q}_a \simeq [2gD\alpha AU_{10}\alpha^2\{(T_{wi} - T_{ai})(c_S + c_L R_H/Be)\} + c_L Leq_s^*(1 - R_H)/C_{pa}]^{1/3}. \tag{A19}$$

For our hot spring parameters (see caption of Fig. 5), the exact solution is $\rho_a \hat{Q}_a = 89.7\, Kgs^{-1}$. Because ε is now 0.31, (A18) is less accurate than our approximate solution (A11) for $\overline{P} = 0$, giving $\rho_a \hat{Q}_a \simeq 98.8\, Kgs^{-1}$. According to (A18), $\hat{Q}_a$ now depends on C_{pa} unlike the $\overline{P} = 0$ case, where $\hat{Q}_a$ is independent of both C_{pa} and C_{pw}. Comparing (A10) with (A17) and (A11) with (A18), we see that precipitation strengthens $\hat{Q}_a$ due to the latent heating of the air that is not present in the $\overline{P} = 0$ case.

We next substitute $Q_a^* = \delta \hat{Q}_a^*$ into a nondimensional version of (A15) to obtain the following expression for the onset asymptotic:

$$\hat{Q}_w^* = (\rho_a C_{pa}^*/\rho_w C_{pw}^*)\{\delta^3 \hat{Q}_a^{*3}/2\hat{T}_w^*\}. \tag{A20}$$

where $\hat{T}_w^*$, consistent with our approximate solution (A17) for $\hat{Q}_a^*$, is given by (A16) without the quadratic term and with $Q_a^* = \delta \hat{Q}_a^*$. The final result is a simple expression for $\hat{Q}_w^*$,

$$\hat{Q}_w^* = (\rho_a C_{pa}^*/\rho_w C_{pw}^*)(c_S^* + c_L^* R_H/Be)\{\delta^3/(1 - \delta^3)\}. \tag{A21}$$

In dimensional form, (A20) becomes

$$\hat{Q}_w \simeq (AU_{10}/2)(\rho_a C_{pa}/\rho_w C_{pw})(c_S + c_L R_H/Be)\{\delta^3/(1 - \delta^3)\}. \tag{A22}$$

For hot spring parameters (Fig. 5) and $\delta = 0.75$, the exact solution for $\rho_w \hat{Q}_w$ is 4.4 $kg\ s^{-1}$, and (A21) gives $\rho_w \hat{Q}_w = 5.6\, kgs^{-1}$. From (A21), we see that to the order of our approximation, $\rho_w \hat{Q}_w$ (*for* $\overline{P} = \overline{E}$) depends only on the ratio (C_{pa}/C_{pw}). Recall that for $\overline{P} = 0$, $\rho_w \hat{Q}_w$ depends on both the ratio (C_{pa}/C_{pw}) and C_{pw}. Again, in the hypothetical limit $C_{pw} \to \infty$, $\rho_w \hat{Q}_w$ decreases to zero for all δ, meaning that there can be no change in any of the variables regardless of the change in Q_w. Comparing (A12) with (A20) and (A13) with (A21) shows that precipitation decreases the asymptotic onset value $\rho_w \hat{Q}_w$; that is, precipitation expands the "domain" of the asymptotic state.

b. Conceptual hot spring model with moisture

i. Hot spring model with moisture and $\overline{P} = 0$. Our problem is to find a reasonable solution to the five extremely nonlinear equations (5), (13), (14), (15), and (16). Note that $\overline{P} = 0$ means there is no latent heating of the air. To make the mathematical problem tractable, we will again take T_{wo} to be known, as opposed to the original "physical" problem where Q_w is known. The five unknowns for our much simpler mathematical problem are Q_w, T_{ao}, Q_a, q_{ao}, and R_{Ho}.

To find the formal solution to our equations, we first solve both (14) and (13) for q_{ao}, giving, respectively,

$$q_{ao} = [(Ac_L U_{10}/2)\{q^*(T_{wi}) + q^*(T_{wo}) - q_{ai}\} + Q_a q_{ai}]/\{Q_a + (Ac_L U_{10}/2)\}, \quad \text{(A23)}$$

$$q_{ao} = [Q_a^2/\beta\{\pi r_0^2 (2gD)^{1/2}\}^2] - \{\alpha(T_{ao} - T_{ai})/\beta\} + q_{ai}. \quad \text{(A24)}$$

Equating (A22) and (A23) gives us the following expression for T_{ao}:

$$T_{ao} = [(1/\alpha)\{Q_a/a(2gD)^{1/2}\}^2 + T_{ai}] + (\beta/\alpha)(Ac_L U_{10}/2)\frac{\{2q_{ai} - (q^*(T_{wi}) + q^*(T_{wo}))\}}{\{Q_a + (Ac_L U_{10}/2)\}}. \quad \text{(A25)}$$

Next, we substitute T_{ao} from (A24) into (5), and, after some manipulation, obtain a *quartic* equation for Q_a,

$$Q_a^4 + k_2 Q_a^3 + k_3 Q_a^2 + k_4 Q_a^1 + k_5 = 0, \quad \text{(A26)}$$

where

$$k_2 = (Ac_S U_{10}/2) + (Ac_L U_{10}/2) \quad \text{(A27)}$$

$$k_3 = (A^2 c_S c_L U_{10}^2/4) \quad \text{(A28)}$$

$$k_4 = (AU_{10}/2)\{\pi r_0^2 (2gD)^{1/2}\}^2[c_S\alpha\{2T_{ai} - (T_{wi} + T_{wo})\} + c_L\beta\{2q_{ai} - (q_s^*(T_{wi}) + q_s^*(T_{wi}))\}] \quad \text{(A29)}$$

$$k_5 = (A^2 c_S c_L U_{10}^2/4)\{\pi r_0^2 (2gD)^{1/2}\}^2[\alpha\{2T_{ai} - (T_{wi} + T_{wo})\} + \beta\{2q_{ai} - (q_s^*(T_{wi}) + q_s^*(T_{wi}))\}]. \quad \text{(A30)}$$

For reasonable choice of parameters, the discriminant Δ is < 0, so there are four distinct roots: two real and two imaginary. Of the two distinct real roots, only one is positive and satisfies all the physical constraints, that is, $0 < R_{Ho} < 1$. Corresponding to the single physical root of (A26), we find solutions of the other unknowns, T_{ao}, q_{ao}, Q_w, and R_{Ho} using (A25), (A24), (16), and (15), respectively.

ii. Hot spring model with moisture and $\overline{P} = \overline{E}$. For this case, the air gains all the heat (both sensible and latent) given up by the hot spring, so equation (5) is replaced by (10).

In addition, $\overline{P} = \overline{E}$ means that equation (14) is replaced by $q_{ao} = q_{ai}$. Similar to the hot spring model without moisture, T_{wo} is known, and Q_a, T_{ao}, Q_w, and R_{Ho} are the four unknowns to be found from (10), (13), (18), and (15). Substituting $q_{ao} = q_{ai}$ into (13) reduces it to (4), which is easily solved for T_{ao}. Next, we substitute $q_{ao} = q_{ai}$ and T_{ao} from (4) into the equation obtained by equating the right-hand sides of (10) and (16). After some simplification, we obtain a cubic equation for Q_a,

$$Q_a^3 + k_2 Q_a^2 + k_3 = 0,$$

where

$$\begin{aligned} k_2 &= (Ac_S U_{10}/2) \\ k_3 &= -(Ac_S U_{10} g D \alpha a^2)[(T_{wo} - T_{wi}) + 2(T_{wi} - T_{ai}) \\ &\quad + (c_L Le/c_S C_{pa})\{q_S^*(T_{wi}) + q_S^*(T_{wo}) - 2q_{ai}\}]. \end{aligned}$$

Again, for reasonable choice of parameters, the determinant Δ is < 0, so there is one real and two complex conjugate roots. Corresponding to the single real root, we find solutions for the other unknowns T_{ao}, Q_w, and R_{Ho} from (4), (10), and (15), respectively.

c. Incompressible atmosphere–ocean model

i. Solution. For mathematical simplicity, we again take Q_a to be given and find solutions for T_{ao}, T_{wo}, D, and Q_w using (5), (6), (24), and (26). Rearranging (26), we obtain the following expression for the temperature of the outgoing air:

$$T_{ao} = T_{ai} + 1/\alpha(\varphi/g)^{1/2}(Q_a/a). \tag{A31}$$

Next, we substitute (A31) into (5) to find that

$$T_{wo} = T_{wi} + 1/\alpha(\varphi/g)^{1/2}(Q_a/a)\{2Q_a/(Ac_s U_{10} + 1\} - 2(T_{wi} - T_{ai}). \tag{A32}$$

Finally, substituting (A31) and (A32) into (6) gives

$$\begin{aligned} Q_w = &\frac{(\rho_a C_{pa}/\rho_w C_{pw})(c_S + c_L R_H/Be) Q_a^2 (\varphi/g)^{1/2}}{c_S \alpha a[2(T_{wi} - T_{ai}) - (Q_a/\alpha a)(\varphi/g)^{1/2}\{(2Q_a/Ac_S U_{10}) + 1\}]} \\ &+ \frac{\{A\rho_a c_L Le U_{10} q_s^*(1 - R_H)\}}{\rho_w C_{pw}[2(T_{wi} - T_{ai}) - (Q_a/\alpha a)(\varphi/g)^{1/2}\{(2Q_a/Ac_S U_{10}) + 1\}]}. \end{aligned} \tag{A33}$$

ii. Incompressible atmosphere–ocean model. In a manner most similar to the analysis of the $\overline{P} = 0$ case for the hot spring model without moisture in Appendix 1a (subsections i and ii), we draw several conclusions from (A32) and (A33). Note that Q_w is positive only for $T_{wo} < T_{wi}$ and decreases monotonically with decreasing Q_a. Conversely, Q_a must decrease with a decrease in Q_w. The ocean transport Q_w has a finite value at $Q_a = 0$ or,

in terms of our original problem, $Q_a \to 0$ at some positive value of Q_w, below which there are no (steady) solutions. For large Q_w, Q_a approaches an asymptotic value $\hat{Q}_a$, as $T_{wo} \to T_{wi}$ from below. In other words, just as in both hot spring models, our incompressible atmosphere–ocean model has the asymptotic state. C_{pa} and C_{pw} control how quickly Q_a reaches $\hat{Q}_a$. In the hypothetical limit $C_{pw} \to \infty$, $Q_a = \hat{Q}_a$ for all Q_w; that is, the system is completely saturated and there can be no change in Q_a (or any of the other variables) regardless of the size of the change in Q_w. All these features of the model are clearly illustrated in Figure 9.

From (A31) and (A32), we see that $(T_{ao} - T_{ai})$ is positive (because Q_a is positive), and, because Q_a decreases with a decrease in Q_w, we see that both T_{ao} and T_{wo} decrease with decreasing ocean transport. Differentiating (A31) and (A32) with respect to Q_a shows that the ocean cools at a faster rate than the atmosphere; that is,

$$dT_{wo}/dQ_a = (\varphi/g)^{1/2}(1/\alpha a)\{1 + 4Q_a/Ac_S U_{10}\} > dT_{ao}/dQ_a = (\varphi/g)^{1/2}(1/\alpha a). \tag{A34}$$

Just as we showed for the hot spring model without moisture, a reduction in the ocean transport causes both the ocean and the atmosphere to cool with the warmer ocean cooling more than the atmosphere (Fig. 11). The resulting reduction in the ocean-atmosphere temperature difference causes a reduction in the sensible and latent heat fluxes (Fig. 10, right panel).

Setting $(T_{wi} - T_{wo} = 0)$ and $Q_a = \hat{Q}_a$ in (A32) yields a quadratic equation for $\hat{Q}_a$,

$$\hat{Q}_a^2 + k_2 \hat{Q}_a + k_3 = 0,$$

where

$$k_2 = (Ac_S U_{10}/2)$$
$$k_3 = -Aac_S U_{10}\alpha(T_{wi} - T_{ai})(g/\varphi)^{1/2}.$$

The (exact) solution for $\hat{Q}_a$ is given by

$$\hat{Q}_a = -(Ac_S U_{10}/4) + [(Ac_S U_{10}/4)^2 + a\alpha Ac_S U_{10}(T_{wi} - T_{ai})(g/\varphi)^{1/2}]^{1/2}. \tag{A35}$$

Using our ocean parameters (see the caption of Fig. 9) and (A35), we find that

$$\hat{Q}_a = 1.78 \times 10^{10} m^3 s^{-1},\ \rho_a \hat{Q}_a = 2.67 \times 10^{10} kg s^{-1}.$$

From (A35), we see that the "asymptotic" value $\hat{Q}_a$ depends on the area of convection region a(radius $= r_0$), the incoming ocean-atmosphere temperature difference $(T_{wi} - T_{ai})$, and the wind speed U_{10}. As seen in Figure 12, increasing any one of these parameters increases $\hat{Q}_a$.

Figure 12 also shows the sensitivity of $\rho_w \hat{Q}_w$, to U_{10}, r_0, and $(T_{wi} - T_{ai})$. Smaller values of U_{10} reduce the asymptotic onset value $\rho_w \hat{Q}_w$, thus expanding the domain of the asymptotic

state, whereas r_0 and $(T_{wi} - T_{ai})$ have only a minimal effect on $\rho_w \hat{Q}_w$. As in all previous $\overline{P} = 0$ cases, $\hat{Q}_a$ is independent of C_{pw} and C_{pa}.

Substituting $Q_a = \delta \hat{Q}_a$ into (A33) yields an expression for the asymptotic onset value $\hat{Q}_w$, which does depend on the specific heat capacities. In particular, larger C_{pw} values give smaller values of $\hat{Q}_w$, expanding the domain of the asymptotic state. For $\delta = 0.75$ and our chosen ocean parameters (caption of Fig. 9), $\hat{Q}_w = 10.5\ Sv$ and $\rho_w \hat{Q}_w = 10.5 \times 10^9\ kgs^{-1}$. Based on this and the sensitivity of $\rho_w \hat{Q}_w$ seen in Figure 12, the asymptotic onset value for our incompressible atmosphere–ocean convection model is estimated to lie somewhere in the range of 8–12 *Sv*.

d. Compressible atmosphere–ocean convection model

i. Solution. Using the same approach that we employed earlier, we simplify the mathematics by taking to be given and solving equations (5), (6), (31), and (32) for T_{ao}, T_{wo}, D, and Q_w. Rearranging (32) gives an expression for the outgoing air temperature.

$$T_{ao} = T_{ai} + (Q_a/a)\{T_{ai}(\gamma_D - \gamma)/2g\}^{1/2} \tag{A36}$$

Next, we substitute (A36) into (5) to obtain

$$T_{wo} = T_{wi} + \{T_{ai}(\gamma_D - \gamma)/2g\}^{1/2}(Q_a/a)\{(2Q_a/Ac_S U_{10}) + 1\} - 2(T_{wi} - T_{ai}), \tag{A37}$$

and finally, substituting (A36) and (A37) into (6) gives

$$Q_w = \frac{[(\rho_a C_{pa}/\rho_w C_{pw})(c_S + c_L R_H/Be)(Q_a^2/aC_S)\{T_{ai}(\gamma_D - \gamma)/2g\}^{1/2}]}{[2(T_{wi} - T_{ai}) - (Q_a/a)\{T_{ai}(\gamma_D - \gamma)/2g\}^{1/2}\{(2Q_a/Ac_S U_{10}) + 1\}]} + \frac{\{A\rho_a c_L LeU_{10} q_s^*(1 - R_H)\}}{\rho_w C_{pw}[2(T_{wi} - T_{ai}) - (Q_a/a)\{T_{ai}(\gamma_D - \gamma)/2g\}^{1/2}\{(2Q_a/Ac_S U_{10}) + 1\}]}. \tag{A38}$$

ii. Compressible atmosphere–ocean model. From our solution, (A36), (A37), and (A38) (shown in Fig. 14), we see the same qualitative behavior that was observed in all our previous models. Q_w decreases with a decrease in Q_a, and, conversely, Q_a decreases nonlinearly with a decrease in Q_w (Fig. 14). For large Q_w, Q_a approaches an asymptotic value $\hat{Q}_a$ (as $T_{wo} \to T_{wi}$ from below); that is, the model has an asymptotic state. C_{pa} and C_{pw} control how quickly the asymptotic state is reached. In the hypothetical limit $C_{pw} \to \infty$, $Q_a = \hat{Q}_a$, for all Q_w, the system is completely saturated and there can be no change in any of the other variables regardless of the size of the change in Q_w. As in all $\overline{P} = 0$ cases, atmospheric convection stops ($Q_a \to 0$) at a positive value of Q_w below which there are no (steady) solutions.

From (A36) and (A37), we see that the decrease in the atmospheric transport in response to a decrease in Q_w results in an increase in the temperature loss of the ocean $(T_{wi} - T_{wo})$

and a decrease in the temperature gain of the atmosphere ($T_{ao} - T_{ai}$); that is, there is a cooling of both the ocean and the atmosphere (see Fig. 15, left panel; and Fig. 16).

Differentiating (A36) and (A37) with respect to Q_a leads to the conclusion that

$$dT_{wo}/dQ_a = \{T_{ai}(\gamma_D - \gamma)/2g\}^{1/2}(1/a)\{1 + 4Q_a/Ac_S U_{10}\} > \tag{A39}$$

$$dT_{ao}/dQ_a = \{T_{ai}(\gamma_D - \gamma)/2g\}^{1/2}(1/a) > 0. \tag{A40}$$

Thus, as in all our previous models, a decrease in Q_w causes the warmer ocean to cool more than the atmosphere. This in turn causes a reduction in both the sensible and latent heat fluxes (Fig. 16 and Fig. 15, right panel).

We next set $(T_{wi} - T_{wo}) = 0$ in (A37) to find $\hat{Q}_a$, the maximum value of Q_a to which the solution asymptotes. This yields a quadratic equation,

$$\hat{Q}_a^2 + k_2\hat{Q}_a + k_3 = 0,$$

where where

$$k_2 = (Ac_S U_{10}/2)$$

$$k_3 = -Aac_S U_{10}(T_{wi} - T_{ai})[(2g/T_{ai})\{1/(\gamma_D - \gamma)\}]^{1/2}.$$

The (exact) solution for $\hat{Q}_a$ is given by

$$\hat{Q}_a = -Ac_S U_{10}/4) + [(Ac_S U_{10}/4)^2 + aAc_S U_{10}(T_{wi} - T_{ai})\{2g/T_{ai}(\gamma_D - \gamma)\}^{1/2}]^{1/2}. \tag{A41}$$

The "asymptotic" value $\hat{Q}_a$ is sensitive to the area of convection region a(radius $= r_0$), the incoming ocean-atmosphere temperature difference $(T_{wi} - T_{ai})$, and the wind speed U_{10} in the same way as the incompressible atmosphere–ocean model; that is, an increase in any one of these parameters causes an increase in $\hat{Q}_a$ (Fig. 17). Figure 17 also shows the sensitivity of $\rho_w\hat{Q}_w$ to U_{10}, r_0, and $(T_{wi} - T_{ai})$. Smaller values of U_{10} reduce the asymptotic onset value $\rho_w\hat{Q}_w$, thus expanding the domain of the asymptotic state, whereas r_0 and $(T_{wi} - T_{ai})$ have only a minimal effect on $\rho_w\hat{Q}_w$. As in all $\overline{P} = 0$ cases, $\hat{Q}_a$ does not depend on the specific heat capacities C_{pw} and C_{pa}. Using parameter values for the North Atlantic (see caption of Fig. 14), we find from (A41) that

$$\hat{Q}_a = 2.06 \times 10^{10} m^3 s^{-1},\ \rho_a\hat{Q}_a = 3.08 \times 10^{10} kgs^{-1}.$$

Substituting $Q_a = \delta\hat{Q}_a$ into (A33) gives an expression for the asymptotic onset value $\hat{Q}_w$, which does depend on the specific heat capacities. As before, increasing C_{pw} reduces the value of $\hat{Q}_w$, thus expanding the domain of the asymptotic state. For $\delta = .75$ and our North Atlantic parameters (caption of Fig. 14), $\hat{Q}_w = 10.6\ Sv$ and $\rho_w\hat{Q}_w = 10.6 \times 10^9\ kgs^{-1}$. Note that this value is virtually identical to the value of $\rho_w\hat{Q}_w$ given by the incompressible

atmosphere–ocean model. Based on this and the similar sensitivity of $\rho_w \hat{Q}_w$ in the two models (Figs. 12 and 17), the asymptotic onset value for *both* our atmosphere–ocean models is estimated to lie somewhere in the range of 8–12 *Sv*.

APPENDIX 2

Symbols used include the following:

a	Area of the convection region (area of window in roof in the hot spring case and actual convection area in the open-ocean case)
A	Total area of the ocean subject to the interaction with the atmosphere
α	Thermal expansion coefficient
β	Moisture expansion coefficient
Be	Bowen ratio
C_{pa}	Heat capacity of air
C^*_{pa}	Nondimensional heat capacity of air
C_{pw}	Heat capacity of water
C^*_{pw}	Nondimensional heat capacity of water
c_S	Sensible heat flux constant
c_L	Latent heat flux constant
c_p	Specific heat at constant pressure
λ	Ratio of the mass transport of air to that of the water
Δ	Determinant
δ	Asymptotic state threshold constant
D	Maximum height to which the air rises
$\overline{E}$	Mean evaporation
F_S	Sensible heat flux
F_L	Latent heat flux
F	Total heat flux
φ	Density gradient
g	Acceleration due to gravity
h	Height to which a parcel rises
k_1, k_2, k_3, k_4	Constants associated with the final algebraic equations
γ	Lapse rate
γ_D	Dry adiabatic lapse rate
L_e	Latent heat of evaporation
ρ_a	Mean density of air over the convection region
ρ_w	Mean density of water in the convection region
ρ'	Density of parcel
ρ	Density of environmental air
$\overline{P}$	Mean precipitation
$P(z)$	Pressure of the environment
$P'(z)$	Pressure of the parcel

q_{ai} and q_{ao}	Specific humidity of incoming and outgoing air
q^*	Saturation specific humidity
Q_a	Transport of the air
Q_a^*	Nondimensional air transport
$\hat{Q}_a$	"Asymptotic" volume flux of atmosphere
Q_w	Transport of water
Q_w^*	Nondimensional water transport
$\hat{Q}_w$	"Onset asymptotic" volume flux of water
r_1	Radius of the ocean's interaction
r_2	Radius of the "convection" region
R	Gas constant
R_H	Relative humidity
$T(z)$	Temperature of the environment
$T'(z)$	Temperature of the parcel
T_{ai} and T_{ao}	Temperature of the incoming and outgoing air over the convection region
T_{ai}^* and T_{ao}^*	Nondimensional incoming and outgoing air temperature
T_{wi} and T_{wo}	Temperature of the incoming and outgoing water
T_{wi}^* and T_{wo}^*	Nondimensional incoming and outgoing water temperature
ε	Small parameter in Appendix 1a (subsection ii)
θ	Potential temperature
μ	Specific volume
U_{10}	Mean speed of atmosphere at 10 m
w	Vertical velocity
W_D	Vertical velocity in the incompressible and compressible models

REFERENCES

Bahadori, M. N. 1978. Passive cooling systems in Iranian architecture. Sci. Am., *238*, 144–154.

Behl, M. 2012. The Robustness of the Heat Released by the Atlantic Meridional Overturning Cell (AMOC) to the Atmosphere. PhD diss. Tallahassee, FL: The Florida State University, Electronic Theses, Treatises and Dissertations (Paper 4714).

Bryden, H. L., H. R. Longworth, and S. A. Cunningham. 2005. Slowing of the Atlantic meridional overturning circulation at 25° N. Nature, *438*, 655–657.

Colin de Verdière, A. 2007. A simple model of millennial oscillations of the thermohaline circulation. J. Phys. Oceanogr., *37*, 1142–1155.

Cunningham, S. A., T. Kanzow, D. Rayner, M. O. Baringer, W. E. Johns, J. Marotzke, H. R. Longworth, et al. 2007. Temporal variability of the Atlantic meridional overturning circulation at 26.5°N. Science, *317*, 935–938.

Curry, R., and C. Mauritzen. 2005. Dilution of the northern North Atlantic Ocean in recent decades. Science, *308*, 1772–1774.

De Boer, A. M. 2010. Oceanography: Sea Change. Nature Geoscience, *3*(10), 668–669.

Hartmann, D. L. 1994. Global Physical Climatology. San Diego, CA: Academic Press, 411 pp.

Hu, A., G. A. Meehl, W. Han, and J. Yin. 2009. Transient response of the MOC and climate to potential melting of the Greenland Ice Sheet in the 21st century. Geophys. Res. Lett., *36*, L10707. doi: 10.1029/2009GL037998

IPCC. 2007. Climate Change 2007: The Physical Science Basis. Contribution of Working Group I to the Fourth Assessment Report of the Intergovernmental Panel on Climate Change. Cambridge: Cambridge University Press, 996 pp.

Kanzow, T., S. A. Cunningham, D. Rayner, J. J.-M. Hirschi, W. E. Johns, M. O. Baringer, H. L. Bryden, et al. 2007. Observed flow compensation associated with the MOC at 26.5°N in the Atlantic. Science, *317*, 938–941.

Knight, J. R., R. J. Allan, C. K. Folland, M. Vellinga, and M. E. Mann. 2005. A signature of persistent natural thermohaline circulation cycles in observed climate. Geophys. Res. Lett., *32*, L20708. doi: 10.1029/2005GL024233

Lozier, M. S. 2010. Deconstructing the conveyor belt. Science, *328*, 1507–1511.

Lozier, M. S. 2012. Overturning in the North Atlantic. Annu. Rev. Mar. Sci., *4*, 291–315.

Lozier, M. S., S. Leadbetter, R. G. Williams, V. Roussenov, M. S. C. Reed, and N. J. Moore. 2008. The spatial pattern and mechanisms of heat-content change in the North Atlantic. Science, *319*, 800–803.

Lozier, M. S., V. Roussenov, M. S. C. Reed, and R. G. Williams. 2010. Opposing decadal changes for the North Atlantic meridional overturning circulation. Nat. Geosci., *3*, 728–734.

Lu, J., S. P. Arya, W. H. Snyder, and R. E. Lawson. 1997. A Laboratory study of the urban heat island in a salm and stuffy stratified environment. Park I. temperature field. J. Appl. Meteor., *36*, 1377–1391

Lu, J., S. P. Arya, W. H. Snyder, and R. E. Lawson Jr. 1997. A Laboratory Study of the Urban Heat Island in a Calm and Stably Stratified Environment. Part II. Velocity Field. J. Appl. Meteor., *36*, 1392–1397

Nof, D., S. Van Gorder, and L. Yu. 2011. Thoughts on a variable meridional overturning cell and a variable heat-flux to the atmosphere. Geophys. Astrophys. Fluid Dyn., *105*, 1–22.

Sandal, C., and D. Nof. 2008. A new analytical model for Heinrich events and climate instability. J. Phys. Oceanogr., *38*, 451–466.

Schmittner, A., M. Latif, and B. Schneider. 2005. Model projections of the North Atlantic thermohaline circulation for the 21st century assessed by observations. Geophys. Res. Lett., *32*, L23710. doi: 10.1029/2005GL024368

Send, U., M. Lankhorst, and T. Kanzow. 2011. Observation of decadal change in the Atlantic meridional overturning circulation using 10 years of continuous transport data. Geophys. Res. Lett., *38*, L24606. doi: 10.1029/2011GL049801

Srokosz, M., M. Baringer, H. Bryden, S. Cunningham, T. Delworth, S. Lozier, J. Marotzke, et al. 2012. Past, present, and future changes in the Atlantic meridional overturning circulation. Bull. Am. Meteorol. Soc., *93*, 1663–1676.

Zhang, D., R. Msadek, M. J. McPhaden, and T. Delworth. 2011. Multidecadal variability of the North Brazil Current and its connection to the Atlantic meridional overturning circulation. J. Geophys, Res., *116*, C04012. doi: 10.1029/2010JC006

Received: *23 July 2012*; revised: *11 September 2014*.